이학박사 학위논문

I. **Efficient and chemoselective reduction using recyclable iron oxide nanoparticles**

II. **Studies on the functionalization and catalytic reactions using Multi-wall Carbon Nanotubes**

I. 산화철 나노 입자들을 이용한 효과적이고 선택적인 재사용 반응

II. 다중벽 탄소 나노튜브를 이용한 표면화와 촉매반응에 대한 연구

2014년 8월

서울대학교 대학원

화학부 유기화학 전공

김 은 석

CONTENTS

Abstract

Part I. Efficient and chemoselective reduction using recyclable iron oxide nanoparticles

Nitro reduction and olefin reduction is one of the most fundamental reactions in organic synthesis. Most common reduction methods used in the laboratories include the use of heterogeneous metal catalysts such as Pd/C, Rh/C, Pt/C, and Raney nickel in the presence of hydrogen gas. We report on the efficient method of olefin reduction using iron oxide nanoparticles.

Commercially available Fe_3O_4 nanoparticles were utilized for the efficient reduction of nitroarenes and olefin reduction using hydrazine hydrate as a hydrogen source. When 20 mol% the nanoparticle catalyst was used for the reduction of nitrobenzene, the catalysts could be recycled 10 times magnetically giving extremely high yields (each 99%) of the reduced product, aniline, without any side products. Excellent chemoselectivity of nitro vs. other reducible functional groups such as halogen, ester, O-benzyl, and N-Cbz groups was also observed. Aliphatic nitro groups were reduced much more slowly with the formation of several side products furnishing moderate yields of aliphatic amines.

Furthermore, Fe_3O_4 nanoparticles were utilized for efficient olefin reductions. Under the optimized conditions, styrene was converted to ethylbenzene in >99% yield within 16 h and various mono- and di-substituted alkenes and alkynes were efficiently reduced to the corresponding alkanes. The catalysts could be recycled 10 times, and Fe_3O_4 catalysts appear almost unchanged in their size and shape.

Using this reduction conditions, alkenes were reduced to the corresponding alkanes with excellent chemoselectivities in the presence of other reducible functional groups such as halogen, O-allyl and O-benzyl groups.

Key words: Nanoparticle, iron oxide, hydrazine, magnetic separation, nitro reduction, olefin reduction

Part II. Studies on the functionalization and catalytic reactions using Multi-wall Carbon Nanotubes

Functionalization of carbon nanotube is essential for its applications. Functionalization of multi-walled carbon nanotubes (MWNTs) was studied using various anchoring methods. Among the reported modification methods for CNT so far, we chose nitrene chemistry and various compounds have been prepared and tested for MWNT modification. Among them, especially nitrene chemistry was employed as the method of choice to preserve desirable physical properties of MWNTs. By using this chemistry, we introduced various linkers such as amine, diamine, hydroxyl amine, and pyridine moieties on MWNTs. And besides We synthesis of carboxyl-functionalized carbon nanotubes (CNTs) was achieved, and then transition metals were incorporated on the linker-MWNT via reductive methods using hydrazine monohydrate.

Among various reducing reagents, the use of hydrazine hydrate allowed us to load palladium uniformly. After immobilization of palladium on CNT, its role as a catalyst for C-C bond coupling reaction (Suzuki reaction) was examined. The catalysts could be retrieved upon completion of the reaction by filtration and drying; the recycled catalysts could then be used in further reactions up to seven times before any loss in catalytic activity was observed. In addition, we report the synthesis of novel Pd-Pt bimetallic nanoparticle catalysts using functionalized multi-wall carbon-nanotubes and utilization of them to reductions. The carbon nanotubes-supported bimetallic nanoparticle catalysts showed improved activity in reduction reactions, compared with that of mono

metal-supported catalysts. Under the optimized reaction conditions, various nitro compounds and alkenes were cleanly reduced at ambient temperature. Furthermore, this catalytic system exhibits excellent activity and high chemoselectivity for nitro compounds in the presence of other functional groups labile to hydrogenation. After the reaction, the catalysts could be collected through filtration, or the used catalysts could be regained by centrifugation and drying, and reused for 10 times without any loss of catalytic activity.

Keywords: Multi-walled carbon nanotube, Heterogeneous catalyst, Suzuki reaction, Recycling, Bimetallic catalyst, Nitro reduction, Olefin reduction

List of Figures

Part I.

Part II.

Figure 6. TEM images of Pd-amine-CNT with Pd

Figure 7. a) H_2 bubbling 30min, b) H_2 bubbling 1h, c) H_2 bubbling 2h, d) $NaBH_4$ 10wt%, e) $NaBH_4$ 25wt%, f) hydrazine monohydrate

Figure 8. a) $NaBH_4$, b) salt adding after H_2 bubbling, c) H_2 bubbling after salt adding

Figure 9. FT-IR of functionalized CNT 1) CNT-pristine, 2) CNT-COOH, 3) CNT-COCl, 4) CNT-ED-OH

Figure 10. TEM image of Pd-CNT-ED-OH catalyst

Figure 11. TEM image of Pd-CNT-ED-OH catalyst after seven reaction cycles.

Figure 12. TEM images of Pd-Pt CNT after 11 times of use

List of Schemes

Part I.

Part II.

List of Tables

Part I.

Part II.

Part I.

Efficient and chemoselective reduction using recyclable Iron oxide nanoparticles

I. Introduction

Catalysts play an important role in industrial applications of direct significance to many aspects such as petroleum refining, fine chemical production, energy conversion and storage[1]. Many catalytic reactions using homogeneous catalysts have been successfully proved, but homogeneous catalysts have recognized to be of somewhat limited use owing to the difficulties in separating the products and impurity by remaining catalyst. Moreover, homogeneous catalysts suffer from the difficult separation of the expensive catalyst from the product for re-use[2]. The homogeneous metal catalysts be inclined to lose their catalytic activity because of metal aggregation and precipitation[3]. These problems are of particular environmental and economic apprehension in large-scale syntheses. Therefore, there has been considerable interest in the development of heterogeneous catalytic systems that can be efficiently re-using system. Hence, heterogeneous catalysts have been extensively employed in various fields because they have fewer of the drawbacks of homogeneous catalysts. The heterogeneous catalysts having metal nanoparticles embedded on metal oxide supports are basic structures that exhibit high activity and efficiency for significant chemical reactions, such as hydrogenation, oxidation– reduction[4].

Especially, among them, iron oxide nanomaterials have attracted great attention. Iron oxide nanomaterials have been found highly applicable and handy in lithium ion batteries, supercapacitors, tissue-specific releasing of therapeutic agents, labeling and sorting of cells, and catalyst[5-8]. Because of their superparamagnetic property and low toxicity, magnetic iron oxide (Fe_3O_4 and g-Fe_2O_3) nanoparticles are especially interesting to biomedical applications, such as diagnostic magnetic resonance imaging (MRI), thermal therapy and drug delivery[9-12]. In my work, I focused on the Iron oxide nanoparticle as heterogeneous catalysts for catalytic applications.

Reduction of nitro group is one of the most essential methods for the preparation of amines, which serve as valuable intermediates for many agrochemicals, pharmaceuticals, dyes, and pigments[13]. Over the past several decades, much effort has been focused on achieving efficient and selective nitro group reduction, and many reaction conditions have been developed for reduction of nitro compounds. Reduction of nitroarenes employing stoichiometric reagents are often associated with undesirable side products, such as hydroxylamine.[14] Therefore catalytic hydrogenation of nitroarenes has been actively pursued employing many readily available metal catalysts such as Cu, Au, Fe, Pd, Pt, and Rh immobilized on solid supports and several hydrogen sources have been utilized including hydrogen gas, silanes and hydrazine derivatives.[15-19] In contrast to the costly metal catalysts mentioned above, iron is one of the most economical and environment-friendly metal catalysts.[20] Since the traditional nitro group reduction using Fe/HCl system (Béchamp process)[21] has been introduced, many iron-mediated catalytic systems have been developed. Homogeneous iron salts have also been used with hydrogen gas or ammonium formate for the nitro reduction. Recently, Lemaire and Beller reported the use of organosilane reagents in presence of homogeneous iron catalysts[22-24]. However, mostly heterogeneous iron catalysts have been used for nitro reduction; iron powders were used with various hydrogen sources such as NH_4Cl, $SnCl_2$, AcOH, and HCl.[25-28]

Hydrazine is an attractive hydrogen source since it obviates the use of autoclaves, acids, and production of large amount of wastes. Reduction with hydrazine hydrate produces harmless by-products such as nitrogen gas and water.[29] After the first report of hydrazine-mediated nitro group reduction over 80 years ago,[30] many heterogeneous catalytic systems involving iron coupled with hydrazine have been reported.[31] Recently we have reported the use of heterobimetallic nanocrystals consisting of Rh and Fe_3O_4 as an efficient

catalyst for nitroarene reduction.[32] However, to the best of our knowledge, there is no report on the nitroarene reduction using commercially available, and easily recyclable superparamagnetic Fe_3O_4 nanoparticle catalyst in presence of hydrazine hydrate.

Also, I carried out olefin reduction using iron oxide nanoparticles. Most common reduction methods used in the laboratories include the use of heterogeneous metal catalysts such as Pd/C, Rh/C, Pt/C, and Raney nickel in the presence of hydrogen gas. As an alternative to the metal-catalyzed hydrogenation, hydrazine mediated olefin reduction has been known for almost one hundred years.[33] The use of hydrazine as a hydrogen source in the olefin reduction has the advantage of not having to resort to the use of a flammable gas and expensive metal catalysts. In the hydrazine-mediated hydrogenation of olefins, it is generally accepted that double bonds are reduced by diimide (NH=NH), which is generated from hydrazine via oxidation.[34] Over the past several decades, many methods of olefin reduction using dimiide precursors have been reported. Although hydrazine decomposition can occur even in the absence of oxidants[35], many strategies have been employed to facilitate the oxidation of hydrazine to diimide. First, instead of hydrazine itself, hydrazine derivatives or diimide precursors such as sodium- or potassium hydrazide, toluene sulfonic hydrazide, azodiformate, or azodicarboxylic acid have been used.[36] Second, additives such as oxygen or hydrogen peroxide and other oxygen equivalent systems have been used often with copper salt, mercury oxide, or potassium ferricyanide.[37] Recently, a broad range of olefin substrates was tested for reduction using hydrazine hydrate with a metal catalyst or through a combination of sodium bromate and acetic acid.[38] From evaluation of literature over several decades, it appears that controlling the speed of diimide generation from hydrazine is a key issue in diimide-mediated olefin reduction. Herein, we report on the mild and convenient method of olefin reduction using iron oxide nanoparticles as an

extremely convenient and recyclable catalyst. Being the most abundant metal on earth, iron is one of the most readily available and environmentally friendly metals. However, there have been scarce reports on simple reduction methods using hydrazine hydrate with iron oxide catalyst for broad spectrum of olefins under neutral conditions.

Generally, magnetically separable catalysts are regarded as one of the most promising heterogeneous catalysts due to their simple recycling process.[39] Among them, magnetic nanoparticles have attracted much attention because it shows good dispersibility and allows an easy recovery after the reaction.[40] Herein, I report on the utilization of commercially available Fe_3O_4 nanoparticles (<50 nm, Aldrich®) for clean, and practical olefin reduction methods.

II. Result and Discussion

Magnetically separable catalysts are very attractive heterogeneous catalysts due to their simple recycling process. Among them, magnetic nanoparticle catalysts have attracted much attention because they show good dispersibility and allow easy recovery after the reaction. Herein, we report on the utilization of commercially available Fe_3O_4 nanoparticles (Aldrich®, <50 nm) towards efficient and selective nitro group reduction.

Table 1. Optimization of nitrobenzene reduction conditions[a]

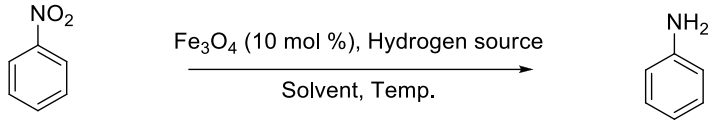

Entry	Hydrogen soruce and solvent	Time (h)	Yield (%)[b]
1	No additive, EtOH	24	0
2	H_2 (1 atm), EtOH	20	0
3	H_2 (1 atm), PPh_3 (10 mol%), EtOH	20	0
4	H_2 (20 atm), EtOH	48	84
5	NH_4O_2CH (4.5 equiv)[c]	20	0
6	NH_4O_2CH (4.5 equiv)	20	0
7	$N_2H_4.H_2O$ (1.5 equiv), EtOH	3(6)[c]	65(99)[c]
8	$N_2H_4.H_2O$ (3.0 equiv), EtOH	3	89
9	$N_2H_4.H_2O$ (4.0 equiv), EtOH	1.5	99
10	$N_2H_4.H_2O$ (4.0 equiv), EtOH	1.5	6[d]
11	$N_2H_4.H_2O$ (4.0 equiv), PhMe	1.5	83
12	$N_2H_4.H_2O$ (4.0 equiv), THF	1.5	26
13	$N_2H_4.H_2O$ (4.0 equiv), DME	1.5	97
14	$N_2H_4.H_2O$ (4.0 equiv), DMF	1.5	99
15	$N_2H_4.H_2O$ (4.0 equiv), H_2O	1.5	14

[a] All reactions were carried out with 1.0 mmol of nitrobenzene in 6.0 mL of solvent at 80 °C unless otherwise noted. [b] Yields were determined by GC analysis using anisole as an internal standard. [c] Yield obtained after 6 h. [d] Reaction was performed at r.t.

First, various hydrogen sources were tested under a variety of reaction conditions employing Fe_3O_4 nanoparticles and the results are depicted in Table 1. Reactions with only the catalyst without any hydrogen source did not proceed at all (entry 1, Table 1). Reactions employing 1 atm hydrogen gas (balloon) in presence of Fe_3O_4 did not proceed regardless the presence of PPh_3 (entries 2 and 3). Reactions at high pressure of hydrogen (20 atm) proceeded rather sluggishly, giving 84% yield after 48 hours (entry 4). When ammonium formate was used as a hydrogen source, no reduction of nitro group was

observed (entries 5 and 6). However, when hydrazine hydrate was used, reduction proceeded smoothly and only 1.5 equivalents of hydrazine was enough to complete the reduction without leaving any trace of incomplete reduction products such as nitroso- or *N*-hydroxylamino-benzene (entry 7). (See Experimental section for GC traces of selected runs) When hydrazine was increased gradually, reactions proceeded faster (entries 7-9) and with 4.0 equiv of hydrazine hydrate the reaction was complete in 1.5 h (entry 9). Temperature was also an important factor; reaction at room temperature produced only 6% yield of the desired product (entry 10). When the reaction was performed in a non-polar solvent such as toluene at 80 ^{o}C (entry 11), product was identified with slightly lower yield. Reaction in refluxing THF produced even lower yield of the product, presumably due to lower reaction temperature (entry 12). When polar aprotic solvents such as DME and DMF were used (entries 13 and 14), nearly quantitative yields of aniline were obtained, therefore the employment of a protic solvent is not a necessity. However, in consideration of cost and ease of solvent removal after the reaction, we chose ethanol as an optimal solvent for nitroarene reduction. Reaction in water proceeded very slowly (entry 15).

Table 2. Reaction dependence on the catalyst amount[a]

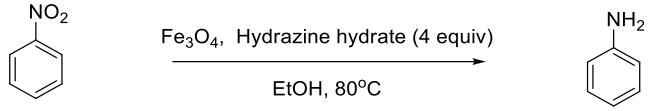

Entry	Amount of Fe_3O_4 (mol%)	Time (h)	Yield (%)[b]
1	0	24	0
2	20	1	99
3	10	1.5	99
4	5	3	99
5	1	6.5	11

[a] All the reactions were carried out with 1.0 mmol of nitrobenzene and 4.0 equiv of hydrazine hydrate in 6.0 mL of ethanol at 80°C. [b] Yields were determined by GC analysis using anisole as an internal standard.

To evaluate the catalytic activity of Fe_3O_4 for nitro reduction, varying amounts of Fe_3O_4 were used. The reaction rate appeared to be dependent upon the amount of Fe_3O_4, and at least 5 mol% of catalyst is required for a practical reduction rate (entries 1-4, Table 2). Reaction using only 1 mol% Fe_3O_4 proceeded very slowly (entry 5).

To examine the scope of substrates for the iron oxide catalyzed reduction, various nitro compounds containing other functional groups such as ester, amide, and halogen have been examined under the standard reaction conditions and corresponding aminoarenes were obtained in quantitative yields within 2 hours (Table 3). It is of particular note that no side product formation was observed in the reactions of compounds containing other reducible functional groups such as *O*-benzyl- or *N*-Cbz-protecting groups (entries 7 and 8, respectively). Based on the fact that hydrazine hydrate is known as two-electron reducing agent,[41] a plausible mechanism of nitro reduction involving the Fe_3O_4 catalyst is suggested in Scheme 1.[42] It is interesting to note that under the Fe_3O_4-catalyzed nitro reduction conditions we detected no nitroso- nor hydroxylamine intermediates on GC analysis. However, in the case of compounds containing a double bond, reduction of the nitro group proceeded along with the double bond reduction (entry 11). This is due to the formation of diimide from hydrazine hydrate, which is

responsible for reducing the double bonds together with the nitro group[41] through two-electron process as shown in Scheme 1.[43] In the reductions of aliphatic nitro compounds (entries 12 and 13), reactivity was noticeably lower than those of aromatic arenes and moderate yields of desired products accompanied by several side products were obtained at prolonged reaction times.

To investigate the origin of the different reactivity of nitroalkanes compared to nitroarenes, we have investigated a set of reactions including both nitroarenes and nitroalkanes. Interestingly, as shown in Fig. 1, it was found that the reduction of nitrobenzene in the presence of nitrohexane ([d]) was considerably slower than the reaction of nitrobenzene alone ([a]). This may indicate that the nitro groups of nitroalkanes bind more strongly to the Fe_3O_4 nanoparticles then do the nitroarenes so that the catalytic reaction on nitrobenzene is slowed down. When nitroalkanes were added during the reduction of nitrobenzene, it was evident that the reactions were slowed down from the moment the nitroalkanes were added ([b] and [c] in Fig. 1). It is intriguing that there was a different degree of inhibition depending upon the nitroalkanes added, namely, the reaction rate was less affected by nitromethane then by nitrohexane. The higher degree of inhibition by nitrohexane might be due to the bulkier hexyl group surrounding the Fe_3O_4 nanoparticles, thus reducing the catalytic activity.

Table 3. Substrate scope of Fe_3O_4 catalyzed nitro group reductions.[a]

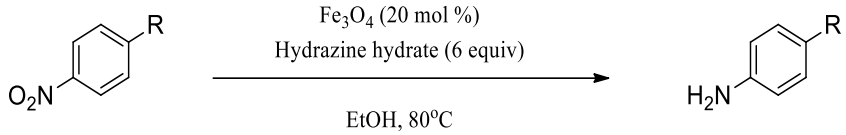

Entry	Substrate	Product	Time (h)	Yield (%)[b]
1	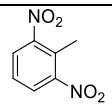	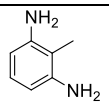	1	99
2	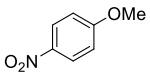	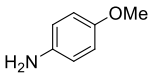	1.5	99
3	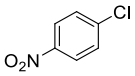	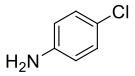	1	99
4	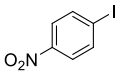	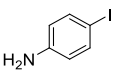	1	99
5	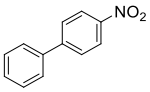	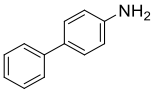	1.5	99
6	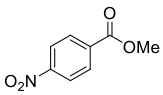	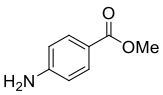	1	99
7	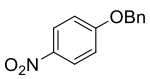	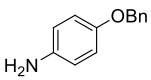	2	99
8	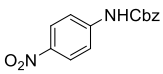	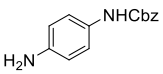	2	99
9	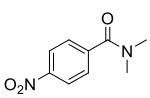	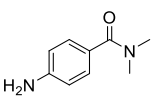	2	99
10	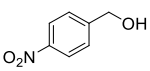	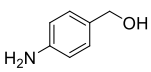	2	99
11	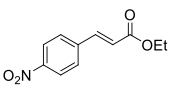	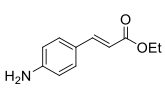	12	45[c]
12	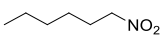	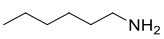	40 18	38 49[d]
13			40	47

[a] Reaction conditions: 1.0 mmol of nitro compound, 6.0 equiv of hydrazine monohydrate, 6.0 mL of ethanol at 80°C. [b] All the yields were determined by GC analysis using anisole as an internal standard. [c] 55% of product was ethyl 3-(4-aminophenyl) propanoate. [d] 10 equiv of hydrazine monohydrate was used.

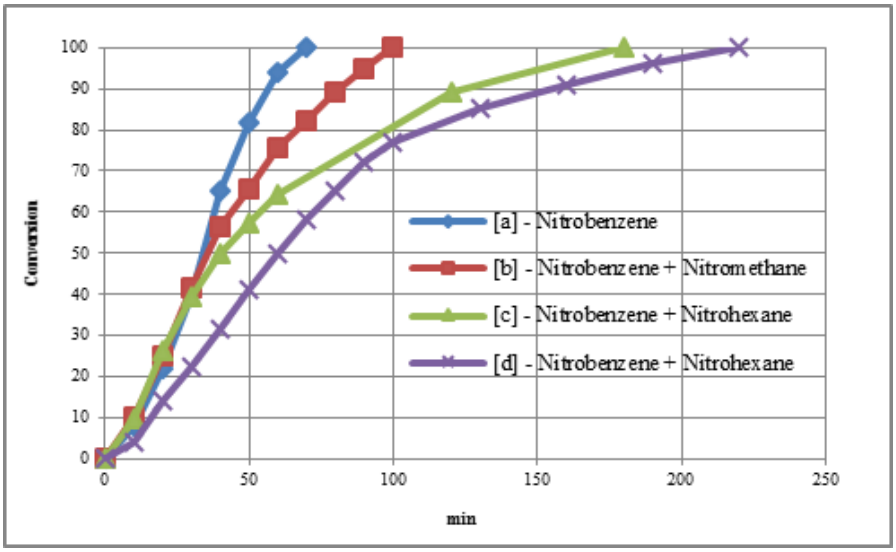

Figure 1. Reaction rate of 20 mol% Fe_3O_4 catalyst in nitrobenzene reduction. [a] nitrobenzene [b] Nitromethane was added in 25 minute. [c] Nitrohexane was added in 25 minute. [d] Nitrohexane was added at first.

With the optimized reaction conditions in hand (10 mol% of Fe_3O_4, 4.0 equiv hydrazine hydrate at 80°C in EtOH), we examined the recycling capacity of the Fe_3O_4 catalyst under optimized reaction conditions taking the reduction of nitrobenzene as a test reaction. After completion of the reaction, the catalyst was collected with an external magnet and the solution was decanted (Figure 2). The remaining catalyst was washed with EtOH and reused for the next set of reaction. As summarized in Table 4, the catalyst showed consistent activity until 5th cycle. Slightly diminished reactivity was observed at 6th run, and prolonging the reaction time secured quantitative conversions at 7th and 8th runs. However, at 9th run yield dropped to 88% even after 7 h reaction. Addition of extra 5 mol% catalyst at the 9th run pushed up the yield to 99%. When we started the recycling reactions with 20 mol% Fe_3O_4 catalyst, however, reactions were complete in an hour and showed no loss of reactivity up to 10 times recycle.

Table 4. Recycling Test of Fe_3O_4 catalyst in nitrobenzene reductions[a]

Catalyst	Run	1st	2nd	3rd	4th	5th	6th	7th	8th	9th	10th
Fe_3O_4 (10 mol%)	Yield (%)[b]	99	99	99	99	95	87	99	99	88	99[c]
	Time (h)	2	2	2	2	2	2	3	4	7	2
Fe_3O_4 (20 mol%)	Yield (%)[b]	99	99	99	99	99	99	99	99	99	99
	Time (h)	1	1	1	1	1	1	1	1	1	1

[a] Reaction conditions: 1.0 mmol of nitrobenzene, 4.0 equiv of hydrazine monohydrate, Fe_3O_4 catalyst in 6.0 mL of ethanol at 80ºC. [b] All the yields were determined by GC analysis using anisole as an internal standard. [c] 5 mol% of additional Fe_3O_4 was added before the reaction.

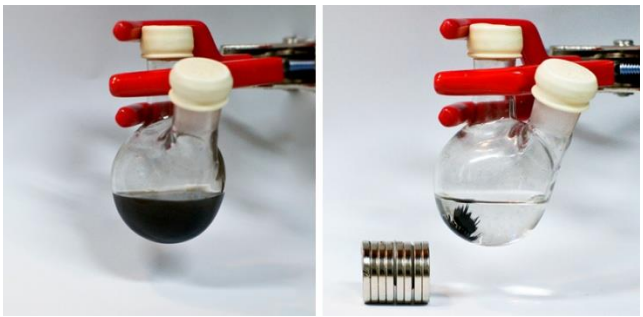

Figure 2. Magnetic separation of Fe_3O_4 catalyst after the reaction

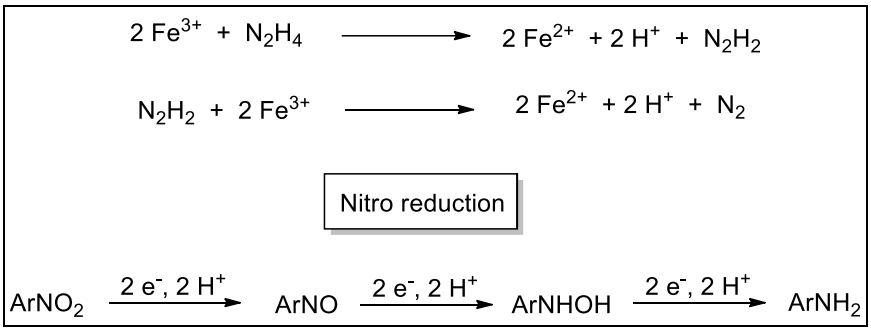

Scheme 1. Proposed mechanism of hydrazine mediated nitro reduction

Figure 3 shows TEM images of Fe_3O_4 catalyst before use and after 10th run with 20 mol% of Fe_3O_4. Although slight aggregation of the nanoparticles was observed, they appear almost unchanged in their size and shape. To see if the

nitro reduction with Fe_3O_4 catalyst can be applied to large scale operations, we scaled up the reaction of nitrobenzene reduction to a 50 mmol scale and ran 10 cycles using 20 mol% catalyst. Each reaction in all 10 cycles was complete in 45 min (see Supporting Information for general procedure and Fe content analysis data).

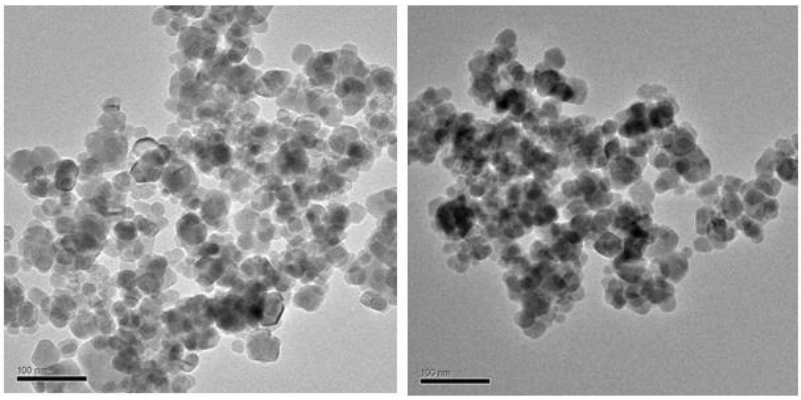

Figure 3. TEM images of Fe_3O_4 nanoparticle before use(left) and after 10 times of use (right)

Next, we estimate the catalytic activity of Fe_3O_4 for olefin reduction. First, we examined the catalytic activity of the Fe_3O_4 nanoparticles taking the reduction of styrene to ethylbenzene as a test reaction (Table 5). Each reaction progress was monitored after 16 h. As can be seen in Table 1, even though the reduction of styrene with hydrazine hydrate proceeded without the Fe_3O_4 nanoparticle catalysts in EtOH at 45 ^oC (45 % yield) and even more (70 % yield) at 80 ^oC (entries 1 and 2, respectively), clearly the presence of Fe_3O_4 nanoparticle catalysts (40 mol %) enhanced the reaction rate of the reduction under otherwise the same reaction conditions and drove the reaction to completion within 16 h (entry 3). The reaction rate appeared to be dependent upon the amount of Fe_3O_4; the reaction using 20 mol % of catalyst was slightly slower than that with 40 mol % and it took 18 h to complete the reaction (entry 4).

Table 5. Optimization of reaction conditions in the reduction of styrene[a]

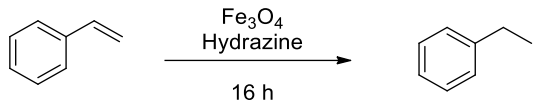

Entry	Fe_3O_4 (mol %)	Hydrazine (equiv)	Solvent	Temp (^oC)	Yield (%)[b]
1	-	8	Ethanol	r.t.	45
2	-	8	Ethanol	80	70
3	**40**	**8**	**Ethanol**	**80**	**99**
4[c]	**20**	**8**	**Ethanol**	**80**	**99**
5	40	8	Ethanol	r.t.	48
6	40	4	Ethanol	80	81
7	40	8	Cyclohexane	80	10
8	40	8	Toluene	80	42
9	40	8	Benzene	80	11
10	40	8	1,4-dioxane	80	18
11	40	8	DMF	80	27

[a] All reactions were carried out with 1.0 mmol styrene in 6.0 mL of solvent for 16 h unless otherwise noted. [b] Yields were determined through GC analyses. [c] The reaction was complete in 18 h.

Consequently, we focused our efforts on the optimization of reaction conditions using 40 mol % catalyst. Reaction at room temperature proceeded very slowly (entry 5) and reaction with 4 equiv hydrazine hydrate was a little slower than that with 8 equiv hydrazine hydrate, giving 81 % yield at 16 h (entry 6). When the reaction was performed in a non-polar solvent such as cyclohexane, toluene or benzene at 80 ^oC, a lower yield was observed presumably due to the lower dispersibility of the iron oxide nanoparticles in the nonpolar solvents (entries 7-9, respectively). Even when a polar aprotic solvent such as DMF was used, a low yield was observed (entry 11). Therefore, we chose ethanol as an optimal solvent for olefin reduction.

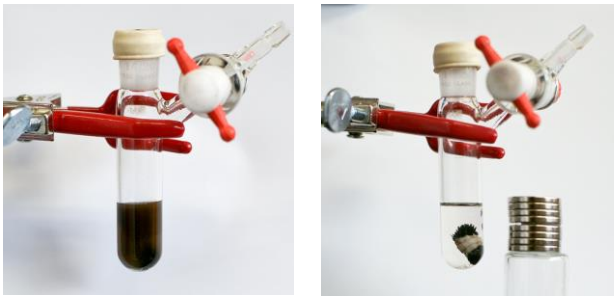

Figure 4. Magnetic separation of Fe_3O_4 catalyst after the reaction.

With the optimized reaction conditions we examined the recycling capacity of the Fe_3O_4 catalyst. After completion of the reaction, the catalyst was collected with an external magnet and the solution was decanted (Fig. 4), then directly analyzed with gas chromatography. The remaining catalyst was washed with ethanol (5 mL x 2), dried under vacuum, and reused for the next cycle of the reaction, and the results are summerized in Table 6. Reactions were complete in 16 h and showed no loss of reactivity up to 10 times recycle.

Table 6. Recycling Test of Fe_3O_4 catalyst in styrene reductions[a]

Run	Time	Yield (%)[b]
1		99
3		99
5	16 h	99
7		99
10		99

[a] All reactions were carried out with 1.0 mmol of styrene in 6.0 mL of solvent at 80°C. [b] Yields were determined by GC.

Based on the results in Table 6, we examined the substrate scope of the new reaction protocol (Table 7). Most of mono- and di-substituted olefins, whether they are aliphatic and aromatic, were reduced to the corresponding saturated compounds in excellent yields.

Table 7. Substrate scope of Fe_3O_4 catalyzed nitro group reductions.[a]

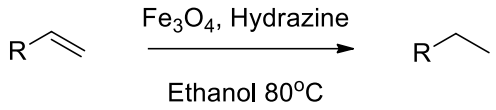

Entry	Substrate	Product	Time (h)	Yield (%)[b]
1	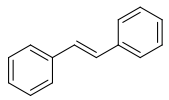	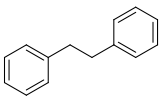	36 (37)	80[d] (87)[e]
2	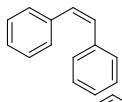	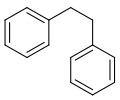	2	99
3[c]	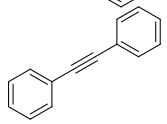	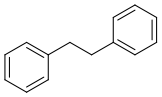	48	65[e]
4	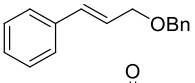	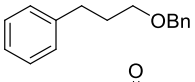	17	99
5	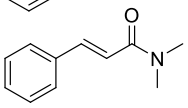	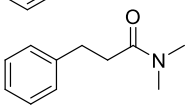	13	99
6	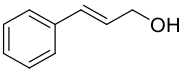	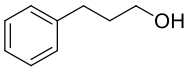	21	99
7	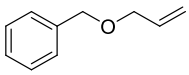	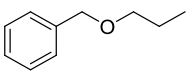	6	99
8			6	99
9	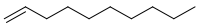	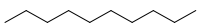	14	99
10			7	99
11	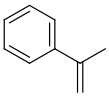	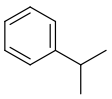	28	99
12	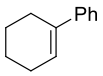	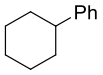	36	21[f]
13	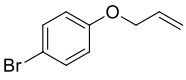	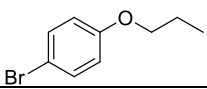	5	93

[a] All reactions were carried out with 1.0 mmol of styrene in 6.0 mL of solvent at 80 °C. [b] Yields were determined through GC analyses. [c] No *cis*-stilbene was detected from GC analysis. [d] 20 equiv hydrazine was used. [e] Reaction was carried out with an additional cosolvent, benzene (2 mL). [f] 12 equiv hydrazine was used.

Both *cis*- and *trans*-di-substituted olefins were reduced efficiently (entries 1-2, 4-11, and 12), although the reduction of *trans*-stilbene was much slower than *cis*-stilbene (entries 1 and 2, respectively). The low reactivity of the *trans*-stilbene may be due to lower solubility of the olefin and addition of benzene as a co-solvent slightly increased the yield (entry 1). Triple bond was also reduced fully to the saturated bond (entry 3), although it took a long time. It is of particular note that no significant amount of side product formation was observed in the reactions of compounds containing other reducible functional groups such as *O*-allyl, *O*-benzyl, and halogen groups (entries 5, 6, 7, and 8). Reduction of di-substituted cyclic olefins proceeded smoothly in 6-7 h to furnish excellent yields of products (entries 10 and 11). Complete reduction of 1,1-disubstituted olefin was observed in 28 h (entry 12), although the reduction of tri-substituted olefin was quite slow even in the presence of 12 equiv hydrazine hydrate, furnishing only 21 % yield after 36 h (entry 13).

To investigate if different reactivities between cis- and trans-olefins and between cis-olefin and alkyne can be utilized in selective reduction of one unsaturated compound over another, we have investigated a set of reactions including both cis- and trans-stilbene, and another set including cis-stilbene and diphenylacetylene (Table 8, entries 1 and 2, respectively). As shown in Table. 4, it was found that a completely selective reduction of cis-stilbene was possible in the presence of either trans-stilbene or 1,2-diphenylacetylene.

Table 8. Different reactivity between *cis*- and *trans*-stilbene and *cis*-stilbene and 1,2-diphenylacetylene[a]

Entry	Substrate	Time (h)	products (%)[b]
1	*cis*-stilbene *trans*-stilbene	2	99 2.6
2	*cis*-stilbene 1,2-diphenylacetylene	2	99 1.6

[a] All reactions were carried out using 1.0 mmol of unsaturated compounds with 40 mol % Fe_3O_4 and 8 equiv hydrazine hydrate in 6.0 mL EtOH and 2 mL benzene at 80 °C. [b] Yields were determined through GC analyses.

III. Conclusion

In conclusion, readily available and magnetically separable Fe_3O_4 nanoparticles were utilized for efficient and recyclable nitroarene reduction. The reaction conditions involving hydrazine hydrate as a hydrogen source are simple and ecofriendly since only nitrogen and water are generated from the reaction and the catalysts can be recycled. All the reductions proceeded in quantitave yields with high reaction rate, and the catalyst was easily separated and reused for the next cycle without any cumbersome filtration process. Furthermore, this catalytic system exhibits high chemoselectivity in nitro reduction in the presence of hydrogenation-labile functional groups. In addition, we have shown that efficient olefin reductions can be accomplished using hydrazine hydrate in presence of Fe_3O_4 nanoparticle catalyst at 80 ^oC in refluxing EtOH. Under the optimized conditions, styrene was converted to ethylbenzene in >99% yield in 16 h and various alkenes and alkynes were cleanly reduced to the corresponding alkanes. Using this reduction conditions, a wide range of di-substituted alkenes was reduced to the corresponding alkanes with excellent chemoselectivities in presence of other reducible functional groups such as halogen, *O*-allyl and *O*-benzyl groups. Consideration that the reaction conditions no hazardous waste was produced, the system offers an efficient way to industrial scale olefin reductions.

IV. Experimental

General

All the reactions were performed by using oven-dried glassware and all commercial materials were used without purification. TLC was performed on aluminum plates with Merck silica gel 60 F_{254}; chromatograms were visualized with UV light (254 and 365 nm). Flash column chromatography was performed on Merck silica gel 60 (ASTM 230-400 mesh). Sonication was performed in a 120 W ultrasonic bath (Branson, B-3210). ^{1}H and ^{13}C NMR spectra were obtained with a Bruker 300 MHz series by using $CDCl_3$ and were referenced to residual TMS peak. GC analyses were performed with a HP-6890 series with a HP-5 capillary column (30 m x 0.25 mm; coating thickness 0.25 μm).

A General Procedure for the recycling of Fe_3O_4 catalyst in nitrobenzene reduction

To an oven-dried, two-necked 25 mL round-bottom flask, magnetic stir bar was equipped. Then Fe_3O_4 (purchased from Aldrich®,46 mg, 0.20 mmol) and ethanol (6.0 mL) were added to the flask, sonicated in an ultrasonic bath for 1 minute. After the flask was equipped with reflux condenser, nitrobenzene (1.0 mmol), anisole (internal standard, 1.0 mmol), and hydrazine monohydrate (200 μL, 4.0 equiv) were added. Then the reaction mixture was stirred at 80°C under argon atmosphere until the reaction was completed. After magnetic separation of catalyst, organic layer was decanted, then directly analyzed with gas chromatography. The remaining catalyst was washed with ethanol (5 mL x 2), dried under vacuum, and reused for the next cycle of the reaction.

Procedure for a large scale nitrobenzene reduction for 10 runs using Fe_3O_4 catalyst

To an oven-dried, two-necked 250 mL round-bottom flask, magnetic stir bar was equipped. Then Fe_3O_4 (purchased from Aldrich®, 2.31 g, 10.0 mmol) and ethanol (150 mL) were added to the flask, sonicated in an ultrasonic bath for 1 minute. After the flask was equipped with reflux condenser, nitrobenzene (5.15 mL, 20.0 mmol), anisole (internal standard, 5.40 mL, 20.0 mmol), and hydrazine monohydrate (10.0 mL, 4.0 equiv) were added. Then the reaction mixture was stirred at 80 °C under argon atmosphere until the reaction was completed. After magnetic separation of catalyst, organic layer was decanted, then directly analyzed with gas chromatography. The remaining catalyst was washed with ethanol (50 mL x 2), dried under vacuum, and reused for the next cycle of the reaction.

Analysis of Fe contents during the recycle (Table 3, entry 2)

- Before use (fresh Fe_3O_4 catalyst): 0.730 wt% of Fe (theoretical value: 0.724 wt %)
- After 10 times of use: 0.755 wt %
- Fe contents in 1st run-reaction extract (20 mL): 3.42 ppm, 0.0680 mg
- > 0.198% of iron leached out in the first catalytic cycle.

Recycling test of Fe_3O_4 catalyst in large scale (50.0 mmol of nitrobenzene)

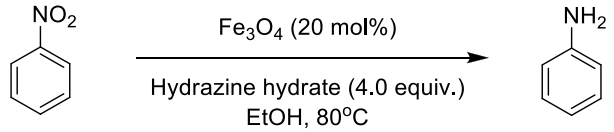

Run	1st	2nd	3rd	4th	5th	6th	···	10th
Time [min]	45	45	45	45	45	45	···	45
Yield [%]	99	99	99	99	99	99	···	99

Representive GC spectrum of nitrobenzene reduction in Fe_3O_4 catalyst recycling test. (Table 4, with 20 mol% of Fe_3O_4)

Nitrobenzene (Starting material)

```
Injection Date  : 9/4/2010 02:45:13 PM
Sample Name     : Nitrobenzene 0.0              Location : Vial 13
Acq. Operator   : KSY
Acq. Method     : KSY-ANILINE.M
Analysis Method : C:\HPCHEM\1\METHODS\BELL_3.M
Last changed    : 2010-11-09 8:05:48 오후
                  (modified after loading)
```

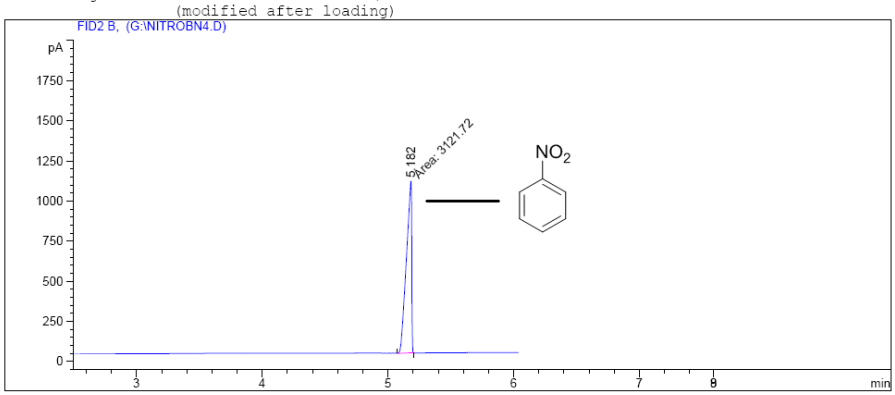

1st cycle (with 20 mol% of Fe_3O_4)

```
=====================================================================
Injection Date  : 9/9/2010 10:00:34 PM
Sample Name     : Fe3O4 nitro red               Location : Vial 17
Acq. Operator   : KSY
Acq. Method     : 07KSY.M
Analysis Method : C:\HPCHEM\1\METHODS\DEF_LC.M
Last changed    : 2010-11-08 8:03:44 오후
                  (modified after loading)
```

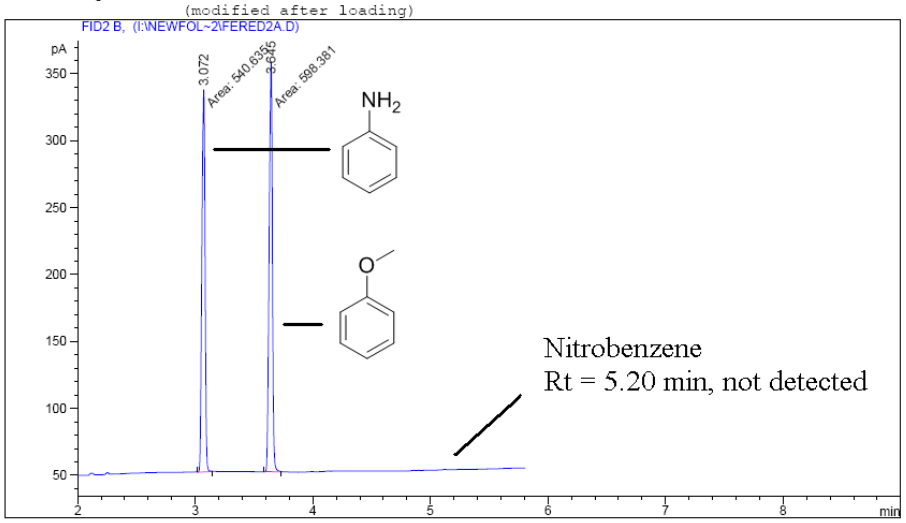

Mass spectrum at Rt = 3.07 min

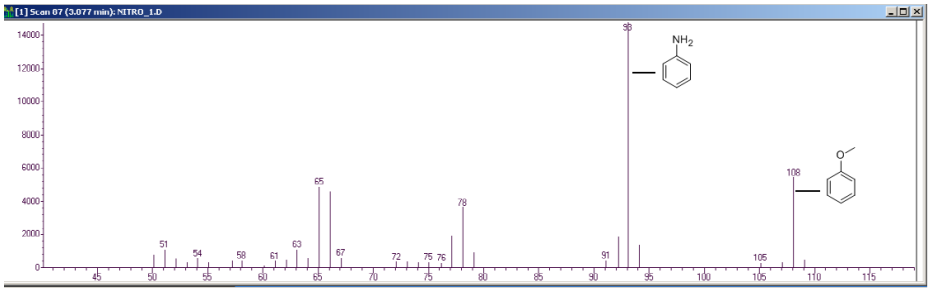

Mass spectrum at Rt = 3.65 min

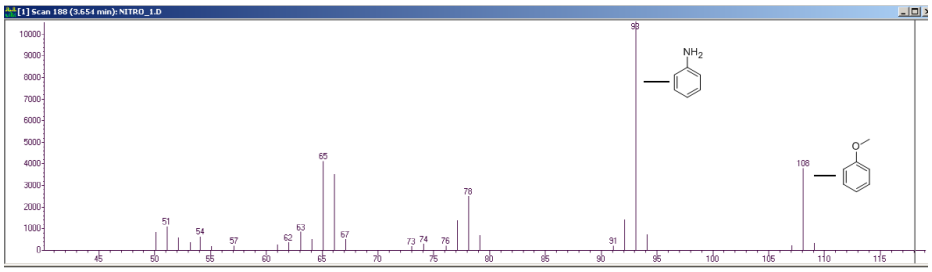

5th cycle (with 20 mol% of Fe_3O_4)

```
Injection Date  : 9/14/2010 03:54:27 AM
Sample Name     : Fe nitro red 5th              Location : Vial 4
Acq. Operator   : KSY
Acq. Method     : 07KSY.M
Analysis Method : C:\HPCHEM\1\METHODS\DEF_LC.M
Last changed    : 2010-11-08 8:06:38 오후
                  (modified after loading)
```

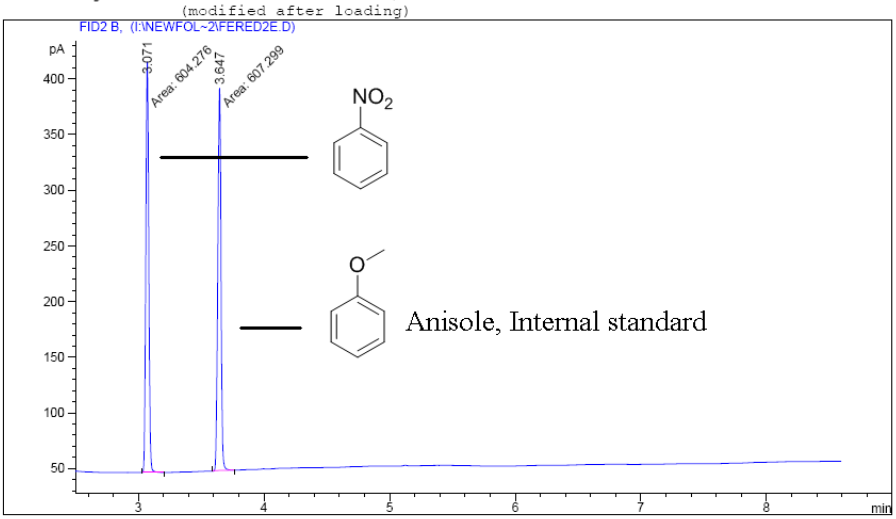

10th cycle (with 20 mol% of Fe_3O_4)

```
Injection Date  : 9/18/2010 03:21:09 AM
Sample Name     : NitroBenzene red                Location : Vial 58
Acq. Operator   : KSY
Acq. Method     : SHK 1029.M
Analysis Method : C:\HPCHEM\1\METHODS\DEF_LC.M
Last changed    : 2010-11-08 8:07:40 오후
                  (modified after loading)
```

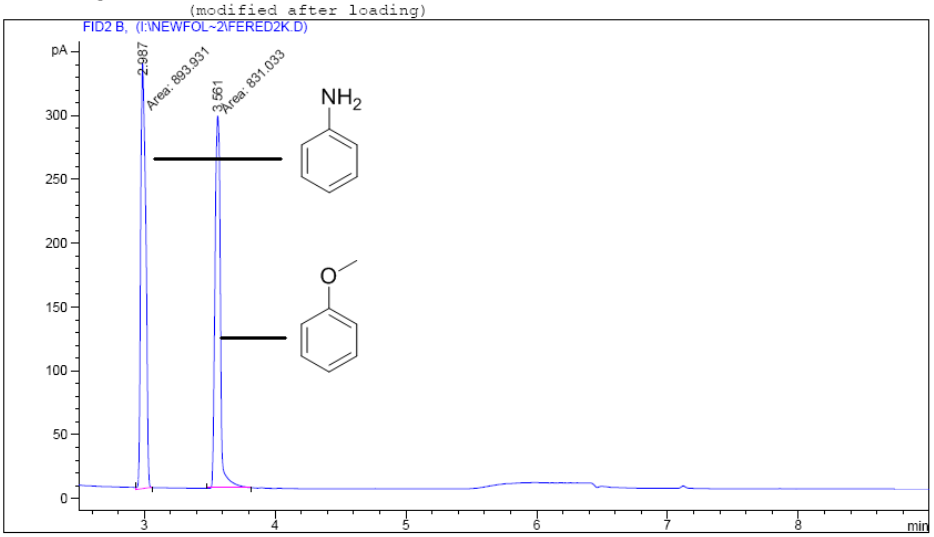

Part II.

Studies on the functionalization and catalytic reactions using Multi-wall Carbon Nanotubes

I. Introduction

Carbon nanotubes (CNTs), first described by Iijima in 1991,[1] CNTs are typical graphene sheets rolled into one dimensional nanotubes with an external diameter ranging between 1 and 100 nm [2]. CNTs can either be single-walled CNTs (SWCNTs) or multi-walled CNTs (MWCNTs), depending on the number of graphene sheets that are rolled up to form them. Especially, CNTs share many attractive characteristics, such as ultrahigh charge carrier mobility, huge thermal conductivity, tremendously large surface area, extraordinary mechanical strength, and flexibility, arising from the purely sp2 hybrid carbon structures with rich delocalized π-electrons.[3–13] These exclusive properties, along with their atomic scale dimension, have caused rapid improvement of various relevant applications, extending from elastic electronics, nanoelectronics, energy conversion/storage, catalysis, to nanocomposites.[14–33]

In this regard, the unique properties make CNTs very useful for supporting metal nanoparticles. Consequently, method for chemical modifications of CNTs have been actively studied. [34] Up to date, numerous methods for CNT functionalization have been reported. They include noncovalent functionalization of SWNTs, such as wrapping of the nanotubes with surfactants, oxidation with strong acids, and direct addition of functional groups with highly reactive intermediates. Among them, commonly used direct covalent modification of CNT sidewall methodologies can be summarized as shown in Table 1.

Table 1. Common CNT sidewall functionalization methods.

Method	Addend	Degree of functionalization	Solubility
Diazonium[35]	Aryl	1 addend/ 10 carbon	0.8 mg / mL in DMF
Diazonium in oleum[36]	Aryl	1 addend /20 carbons	0.25 mg / mL in H2O
Fluorination[37]	Fluorine	1 addend / 2 carbons	1 mg / mL in 2-propanol
Radical chemistry[38]	Alkyl	1 addend / 6 carbons	-
Dissolving metal reduction[39]	Alkyl, aryl	1 addend / 17 carbons	-
Azomethine ylide (Prato reaction)[40]	Pyrrolidine	1 addend / 100 carbons	50 mg / mL in DCM
Nitrene[41]	Aziridine	1 addend / 50 carbons	1.2 mg / mL in DMSO
Bingel reaction[42]	Cyclopropane	1 addend / 50 carbons	-
Dichlorocarbene[43]	Cyclopropane	1 addend / 25 carbons	-

Non-covalent functionalization is based on attraction of the hydrophobic end of an adsorbed molecule to CNT walls via van der Waals forces or π–π interactions[44]. This type of functionalization can be performed in ionic liquids and does not inhibit the electronic structure of CNTs. The main drawback of non-covalent bonding is that it is difficult to control the functionalization system and characterize the product.

Covalent functionalization includes formation of covalent bonds between numerous functional groups and the sidewalls or defect sites on tips of CNTs. Covalent functionalization can be achieved by fluorination of CNTs,

cycloaddition, boron adsorption and nitrogen adsorption via HNO_3, HNO_3/H_2SO_4 or diazonium salt. Cycloaddition can be achieved through various reactions like 1,3-dipolar cycloaddition of azomethineylides, carbene [2+1] cycloaddition or Diels–Alder reaction via microwave irradiation cycloaddition.[45] Also, Common methodologies of direct covalent modification include radical chemistry, Prato and Bingel reactions, as well as dichlorocarbene and nitrene chemistry.[46]

To prepare functionalized CNTs, we have used some functionalization methods to change the sidewalls of MWNTs. We chose to further explore the reactive nitrene chemistry as a functionalization method, since only desired functional groups of the reactive species can be attached to the CNT wall without considerably damaging CNTs. Generation of nitrene is performed in situ from an azide moiety to minimize undesirable additions such as insertions or rearrangement reactions. Aziridine rings can be formed as reported in studies examining nitrene chemistry.[47-49] Several functional groups were attached to the azido linker and transition metals were loaded on MWNTs for use in catalytic systems.

All our works on CNT were carried out using multi-walled nanotube (MWNT), which was prepared by chemical vapor deposition (CVD) method. Although properties of single and multi-walled nanotubes may different in many points including their reactivity, we assumed that functionalization method for SWNT can be applied to MWNT.

Meanwhile, among numerous functional groups, carboxylates are the most commonly employed for the immobilization of enzymes, ligands, and sensors on CNT.[50-57] Since carboxylated CNT’s can stabilize metal nanoparticles, these materials have also been used for the incorporation of transition-metals on CNT (Pd, Pt, Ru, Rh, Au, Ni, Cu).[58-62]

A key issue in loading noble metals onto CNTs is the surface area of metal nanoparticles and their dispersion on CNTs. Good value catalysts should have a high metal surface area/volume ratio and high dispersion[63]. However, pure CNTs have not enough binding sites to support in fixing of metal nanoparticles leading to poor metal dispersion. To increase metal dispersion and decrease aggregation, it is necessary that CNTs be functionalized with polar groups (such as hydroxyl and carboxylic groups) prior to metal loading [64]. Therefore we tried to synthesize metal nanoparticle CNTs using carboxylated CNTs. Though examples on the use of Pd-CNT catalyst systems abound in the literature, reports on the use of the heterogeneous Pd-CNT systems for recyclable and highly reactive catalyst systems are rare.[65-71] Hence, a novel Pd-CNT catalyst was prepared through the incorporation of a new ligand system and its performance as a recyclable catalyst in the Suzuki reaction was investigated.

In addition, over the last few years, many studies have been reported on bimetallic nanoparticle catalysts.[72–74] Compared with monometallic nanoparticles, bimetallic nanoparticles show interesting electronic, optical, chemical or biological properties because of not only their developed catalytic activity but also their novel properties.[75,76] Bimetallic nanoparticles are commonly synthesized using polymers and surfactant stabilizers such as polyvinylpyrrolidone (PVP) and quaternary ammonium salts.[77-80] However, since such polymers and stabilizers can reduce the catalytic activity, there is a growing need for the development of new methods for synthesizing well-dispersed bimetallic nanoparticles on solid supports.

A recent report has demonstrated that well-dispersed metallic nanoparticles on CNT supports show high catalytic activities and recyclability for hydrogenation.[81] Therefore, carbon nanotubes are suitable supports for metal nanoparticle systems[82-86] involved in redox reactions. Reduction of the nitro

group is one of the convenient organic reactions for the preparation of amines, which are fundamental compounds for the synthesis of many agrochemicals, pharmaceuticals, dyes, rubbers, polymer, and pigments.[87] Since reduction of nitro compounds using stoichiometric reagents often produces unwanted side products such as hydroxylamine,[88] researchers have searched for efficient and selective nitro-group reduction methods including metal-catalyzed reactions. Since the introduction of Béchamp process,[89] Corma and Serna reported that gold nanoparticles supported on TiO_2 catalyzed chemoselective reduction of functionalized nitroarenes with H_2. Many metal catalysts such as Cu, Au, Fe, Pd, Pt, and Rh immobilized on solid supports have been utilized for reduction of nitro compounds in combination with hydrogen sources, including H_2, silanes, and hydrazine derivatives.[90-93] From our continuing efforts on the study of the bimetallic nanoparticles, I carried out chemoselective reduction of nitro compounds.[94]

II. Result and Discussion

Although many functional groups can be introduced with above methods, the reaction processes are slightly hazardous and cumbersome.

After a few times of trial, we modified and optimized the reaction conditions of diazonium method for MWNT functionalization. In these conditions, isoamyl nitrite was used for diazonium salt generation and sufficient amount of solvent was used (about 50 mL of 1,2-dichlorobenzene was used per 50 mg of MWNT). First, we carried out reactions with 4-nitroaniline to verify introduction of functional group on CNT by infrared spectroscopy using the optimized conditions (Scheme 1). As a result, after the reaction and drying under vacuum, a distinguishable IR pattern of nitro group (~1340 cm^{-1} and 1520 cm^{-1}) appeared (Figure 1).

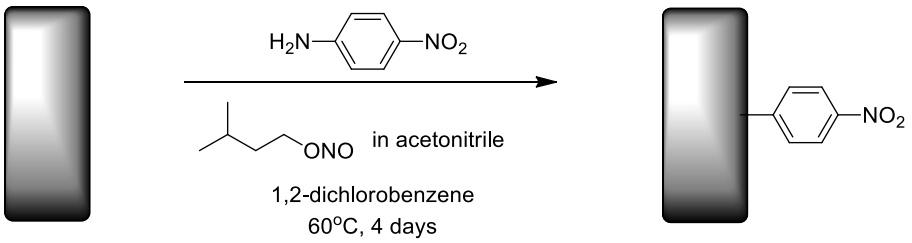

Scheme 1. Functionalization of MWNT with 4-nitroaniline using diazotization.

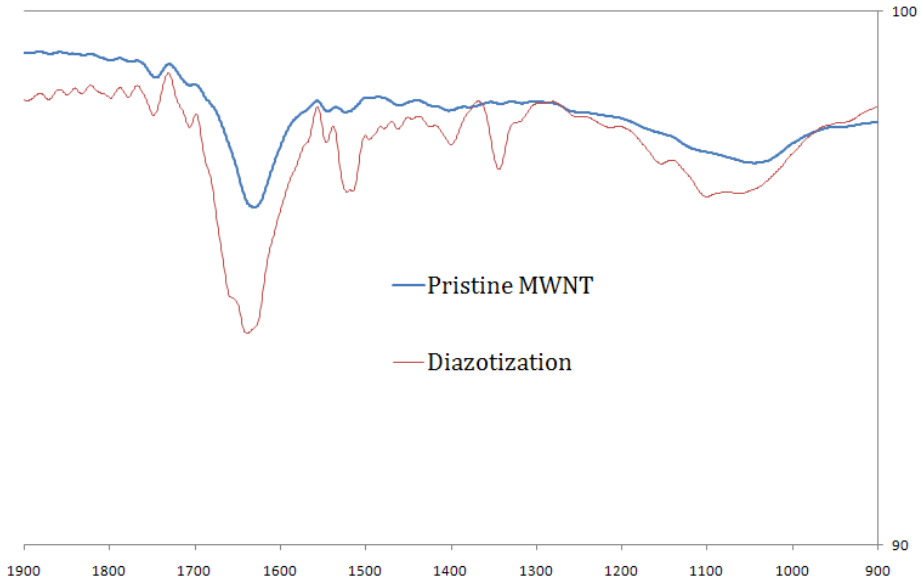

Figure 1. IR spectrum of pristine MWNT and introduction of 4-nitrophenyl.

After the reaction, mass of MWNT material was increased by about 40%. To identify the degree of functionalization, the MWNT material obtained from the reaction was analyzed by elemental analysis (C, H, N) and compared with the result of pristine MWNT (Table 2).

Table 2. Elemental analysis of MWNT before and after diazotization.

Sample name	Nitrogen	Carbon	Hydrogen
Pristine MWNT	N.D.	84.1466%	0.2395%
After Diazotization	2.8844%	78.6369%	1.0917%

Based on nitrogen content analysis of the MWNT, it was estimated that the nitrophenyl group was introduced in about every 300 carbon atoms. Although the degree of functionalization is slightly lower than those of SWNTs', in consideration of MWNT's relatively low surface area/mass ratio, functionalization ratio was considered to be comparable to references in Table 1.

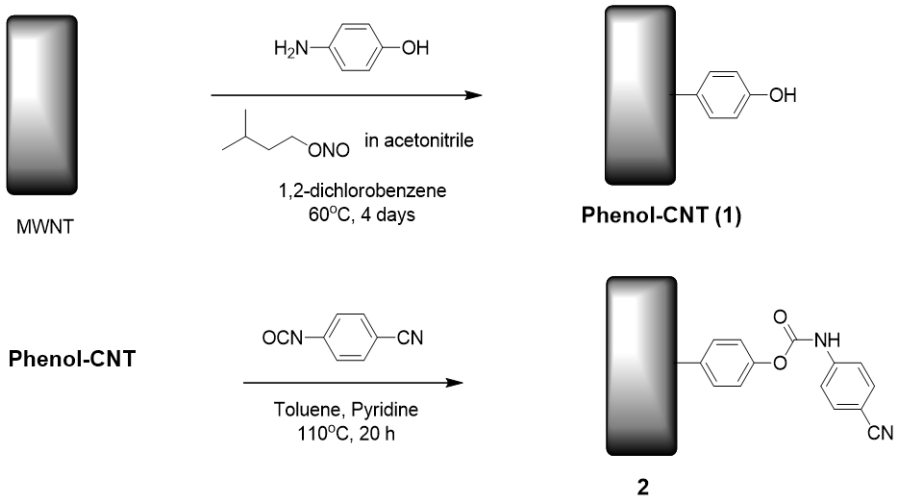

Scheme 2. Introduction of hydroxyl group and further functionalization using 4-cyanophenyl isocyanate.

We decided to apply preparation methods for the introduction of other functional groups such as nitrile and hydroxy group onto the nanotube. Especially, when phenol group is successfully immobilized on sidewall of CNT, bottom-up approach is possible utilizing hydroxyl group for further modification of CNT. Using similar reaction conditions, 4-aminophenol was allowed to react with MWNT through an intermediate diazonium salt. After the reaction, product of slightly increased mass (60 mg -> 63 mg) was obtained, and bands corresponding to a hydroxyl group (~1100 cm^{-1} and 1250 cm^{-1}) were identified in IR spectrum. Consequently, the product was treated

with 4-cyanophenyl isocayate for testing the reactivity of the introduced hydroxyl group. MWNT material was sonicated in toluene, then the suspension was heated under argon at 110 ^{o}C with excess (~1000 wt %) isocyanate and pyridine (Scheme 2).

Carbamate formation and the presence of nitrile group were identified in IR spectrum as shown in Figure 2. Peaks corresponding to the nitrile (2220 cm^{-1}) and carbamate (1630 cm^{-1}) groups and a band for para-substitution on phenyl (~800 cm^{-1}) were identified. Resulting material showed enhanced dispersibility in some organic solvents such as DMF (~ 10 mg / 50 mL).

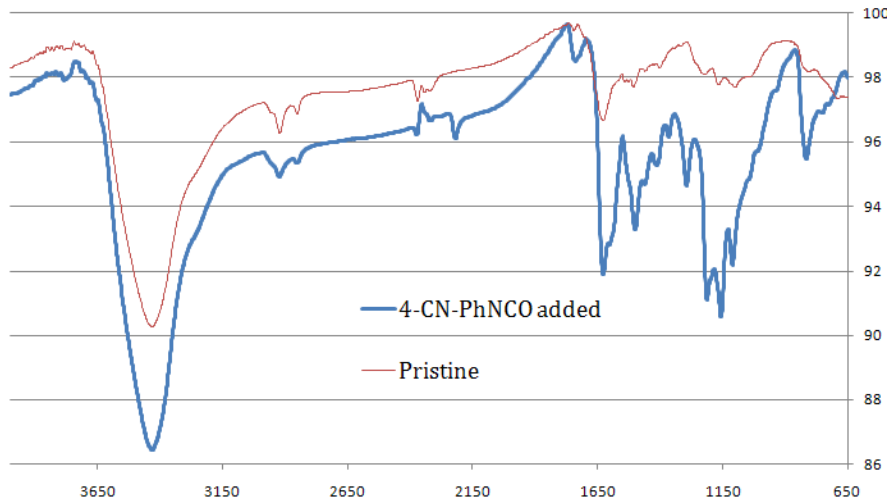

Figure 2. IR spectrum of functionalized MWNT after carbamate formation.

With these experiments, possibility of bottom-up approach for MWNT modification using multi-step functionalization was confirmed. However, when these modified materials were used for further applications, thermal stabilities of carbamate, ether, and ester linkages were considred to be doubtful. Therefore, we decided to extend structures on MWNT sidewall using carbon-carbon bond formation such as Suzuki-Miyaura coupling. For this purpose, 4-bromophenyl moiety was employed for preparation of

halogen-containing MWNT. Resulting material also showed good dispersilibility in DMF and acetone. After the identification of IR spectrum changes, two batches of Suzuki coupling were carried out with cyano- or nitrophenylboronic acid in order to verify potential for further functionalization using cross-coupling reacation (Scheme 3)

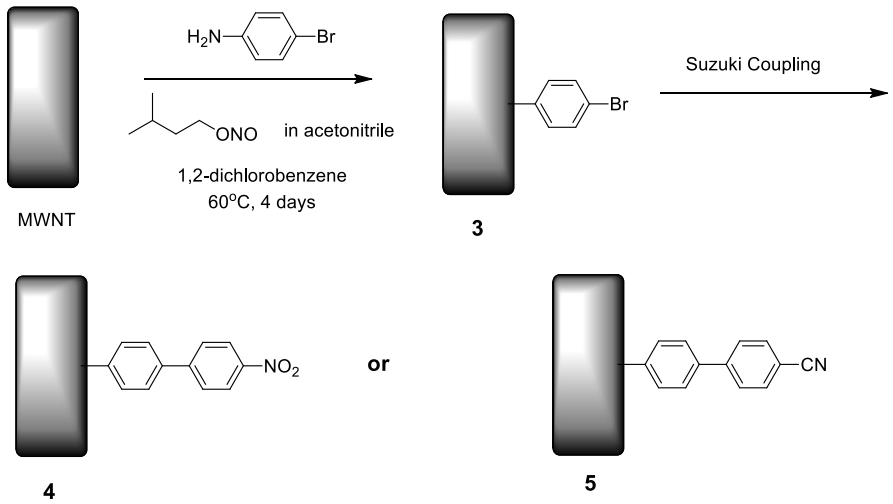

Scheme 3. Introduction of 4-Bromophenyl group and further modification using Suzuki coupling.

From these experiments and analysis, we verified that multi-step functionalization is possible approach for the modification of MWNT, however, the degree of functionalization does not appear to be enough for further applications such as reduction of the nitrile or nitro group to access to an amine moiety. Therefore, it is clear that a broad range of reaction conditions is needed for denser functionalization of the CNT sidewall. As an alternative method, we decided to try other functionalization approaches.

We chose nitrene chemistry as an alternative functionalization method. In this method, reactive intermediate is generally formed *in situ* from an azide. Dependent on the neighbouring group, generated nitrenes can add, insert or

rearrange.[43] Two species of nitrenes are generated after thermal or light induced extrusion of N_2: singlet-state and triplet-state nitrenes. The singlet nitrenes have two p-orbitals, each filled with two electrons. They can either attack the nanotube sidewall in an electrophilic [2+1] cycloaddition or undergo a transition into a triplet-state by inter-system crossing (ISC). A triplet-state nitrene has one filled p-orbital and two porbitals with un-paired electrons. Thus, triplet-state nitrenes are biradicals and they could therefore react with the π-system of the nanotube sidewalls. In both cases aziridine rings can be formed (Figure 3).

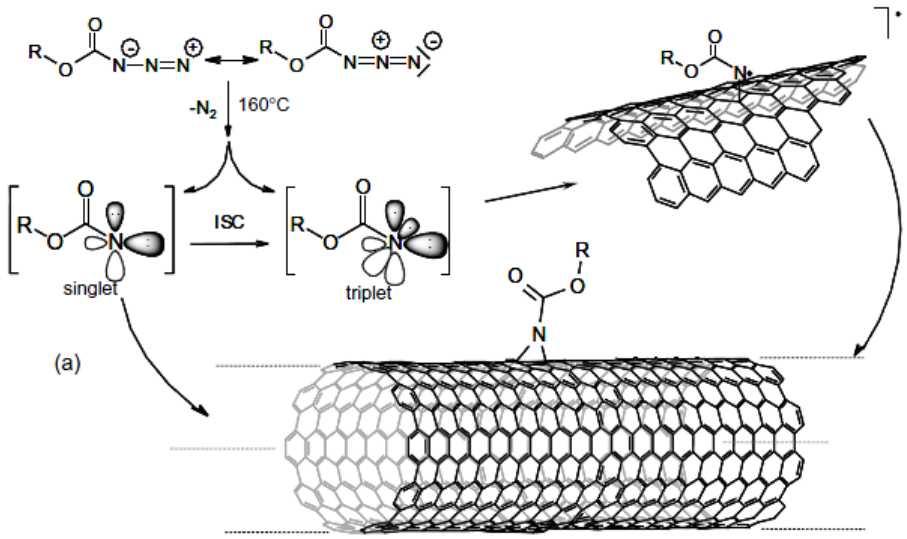

Figure 3. Schematic presentation of the reaction of nitrenes with the nanotube sidewall.

In most reports dealing with the nitrene chemistry, nitrene compound was generated from azidocarbonate esters which can easily be synthesized from alcohols in a two step reaction. However, for the ease of simpler preparation of various nitrene precursors, we attempted to use alkyl- or aryl azide for CNT functionalization for the nitrene chemistry.

For our modification of MWNT, new properties of functionalized MWNT's are of a key concern, therefore we decided to use them as criteria for our MWNT modification. First of all, to verify enhancement of dispersibility in organic solvent, we synthesized a long-chain alkyl azide and performed nitrene reaction with MWNT. About 200-fold of dodecyl azide was used for the reaction (Scheme 4). The material obtained from this reaction, **6**, did not show any mass increase, nor any change in IR spectrum. However, compound **6** showed great enhancement of dispersibility in polar aprotic solvents such as dichloromethane (1.0 mg/10 mL) with a relatively low degree of functionalization (1 per every 14,500 carbon atoms based upon elemental anaylsis).

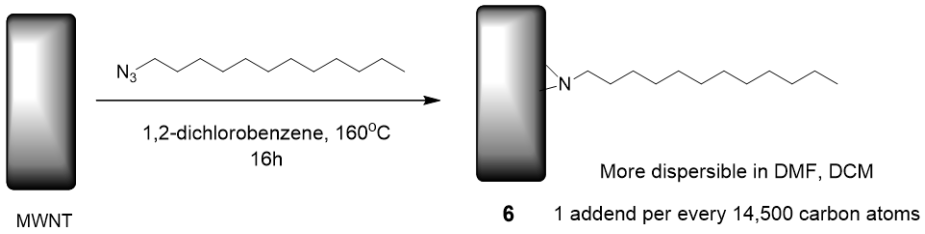

Scheme 4. Introduction of dodecyl chain using nitrene chemistry.

Encouraged by this result, we attempted to prepare two groups of azide compounds; an azide containing either a leaving group or a nucleophile. With these two types of azide compounds, it was envisioned that a wide range of nuclophiles and electrophiles could be introduced to bring about expansion of MWNT derivative applications.

For simple covalently attached structure on MWNT, we synthesized alkyl azides containing a leaving group and tried to immobilize it on the MWNT sidewall. As shown in Scheme 5, bromide, tosylate, and terminal olefins were selected as a leaving group or an electrophile to be carried on in nitrene chemistry with MWNT. However, after reactions with the MWNT, most of

the resulting compounds were stiff solids and mass of the products were heavily increased. Moreover, these materials could hardly be dispersed in most of organic solvents and there is no appearance of new bands which can be assigned to tosylate, bromide or terminal olefin. From the NMR analysis of the filtrate, we assumed that electrophile-containing azide compounds were converted to nitrene during the reaction, and consequently they were involved in the reaction with other azide compounds containing leaving groups. In this manner, self-elongation or polymerization might have occurred, then these compounds were possibly absorbed on MWNT surface.

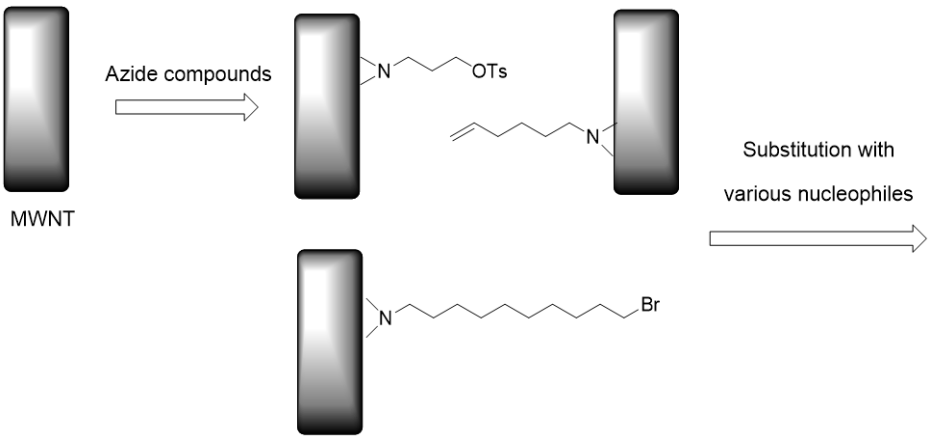

Scheme 5. A plan for the preparation of electrophile-containing MWNT and further reactions with nucleophiles.

As a second route to the MWNT functionalization using nitrene chemistry, azide compounds containing a terminal alcohol, a carboxylate, or an amino group were prepared and used for the reaction with MWNT. Because these compounds are more stable than compounds containing leaving group, it was envisioned that there might be less chance for polymerization during the reaction. In addition, it was anticipated that the terminal functional groups

such as alcohol, carboxylate, and amino groups may lead to a reduction of van der Waals interactions between the CNTs and render the MWNT more dispersible in organic solvents.

The introduction of carboyxlate groups on CNT is commonly done by immersing CNT in strong acids[95] such as nitric acid, sulfuric acid, hydrochloric acid or their mixture. Use of alternative acids have also been studied and used to oxidize CNT. In these methods, a mixture of H_2SO_4/HNO_3 (3:1)-H_2O_2, phosphorous pentoxide (P_2O_5)–polyphosphoric acid, sulfuric acid-potassium dichromate have been used.[96-98] However, most of these methods have been aimed at the creation of defect sites on MWNT followed by functionalization from the oxidized defects. This inevitably brings perturbation on CNT structure and effect physical and chemical properties of CNT.

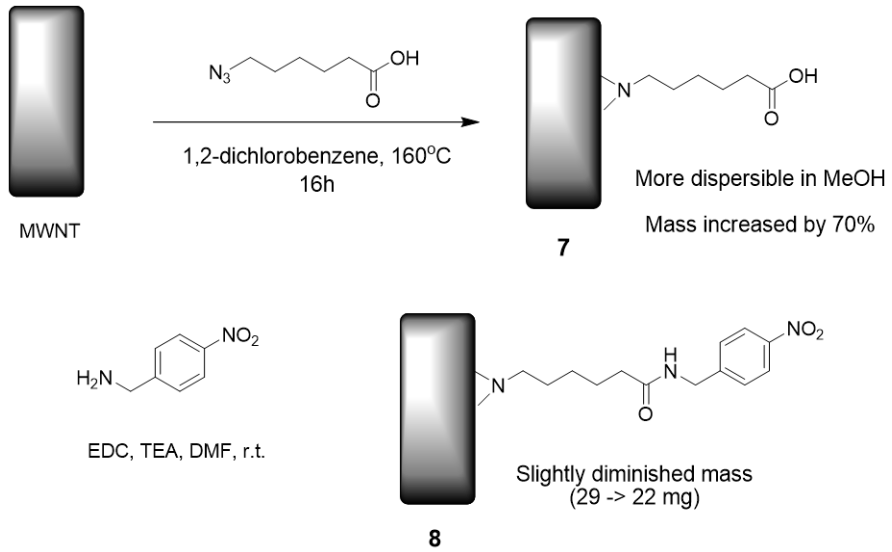

Scheme 6. Two-step approach for introduction of aliphatic carboxylic groups and amide bond formation on MWNT.

On the other hand, if carboxylate group is introduced by nitrene chemistry, sidewall of CNT receives little damage from functionalization. Therefore, if functionalization of MWNT with nitrene chemistry using azidoalkyl chains containing carboxylate, alcohol, and amino functionalities can successfully be done, it would be a very useful method for the introduction of functional groups on CNTs and thus constitute a nice bottom-up approach for further applications.(Scheme 6)

Therefore we tried several trials, many other azide compounds were used for nitrene chemistry for MWNT functionalization. Results of trials not mentioned above are summarized in Table 3.

Table 3. List of used azide compounds and results of nitrene reaction.

Entry	Compound	Functional group	Change in mass	IR spectrum / *dispersibility*
1	1-Azido-8-octene	Terminal olefin	+200%	-
2	1-Azido-3-propionitrile	Nitrile	-	-
3	4-Nitrobenzyl azide	Nitro	-	-
4	1-Azido-6-hexanioic acid methyl ester	Ester	+15%	Carbonyl band-
5	THP protected azido propanol	Alcohol	+30%	-
6	1,5-Diazidopentane	Azide	+ 5~ 10%	Very weak azide band
7	Tetraethylene glycol-azide	PEG / alcohol	Over + 200%	*Well dispersible in Methanol, DCM*
8	Nosyl azide	Nitro	Over +200%	Strong nitroband

Although several methods have been used so far, high degree of functionalization and further modicifation of MWNT has not been achieved. As a last resort, for the introduction of an aliphatic amine on MWNT surface, we prepared 5-azidopentylamine and its derivative as shown in scheme 7.

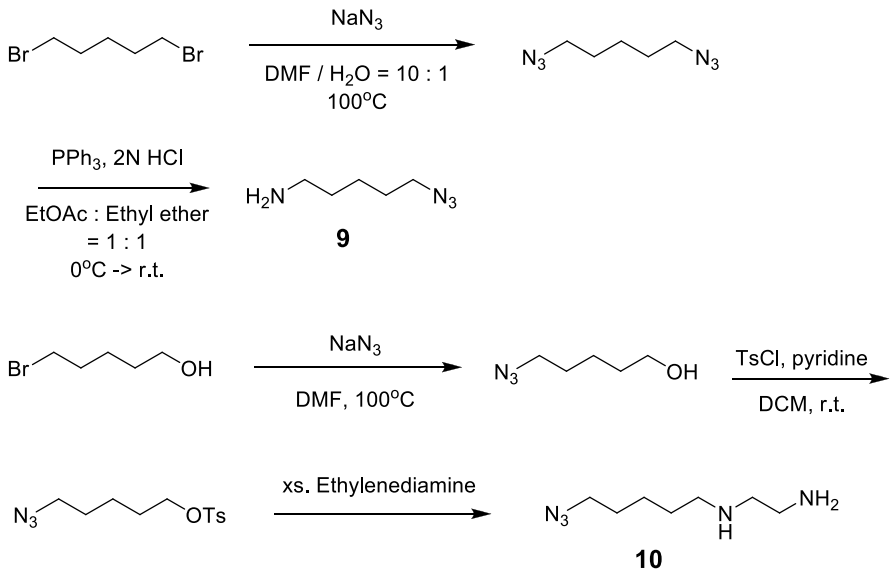

Scheme 7. Preparation of 5-azidopentylamine and its ethylenediamine adduct

With these compounds, nitrene chemistry was carried out onto MWNT. Each 100 mg of MWNT was treated with 1,000 wt% of amine-azide compound **9** or **10** in 1,2-dichlorobenzene, and the reaction furnished agglomerate, which showed two- or three-fold mass increase (Scheme 8). Fortunately, the materials obtained from this reaction were highly dispersible in most solvents, especially in water (10 mg / 50 mL). The TEM images of water dispersed **9-a** and **10-a** are shown in Figure 4.

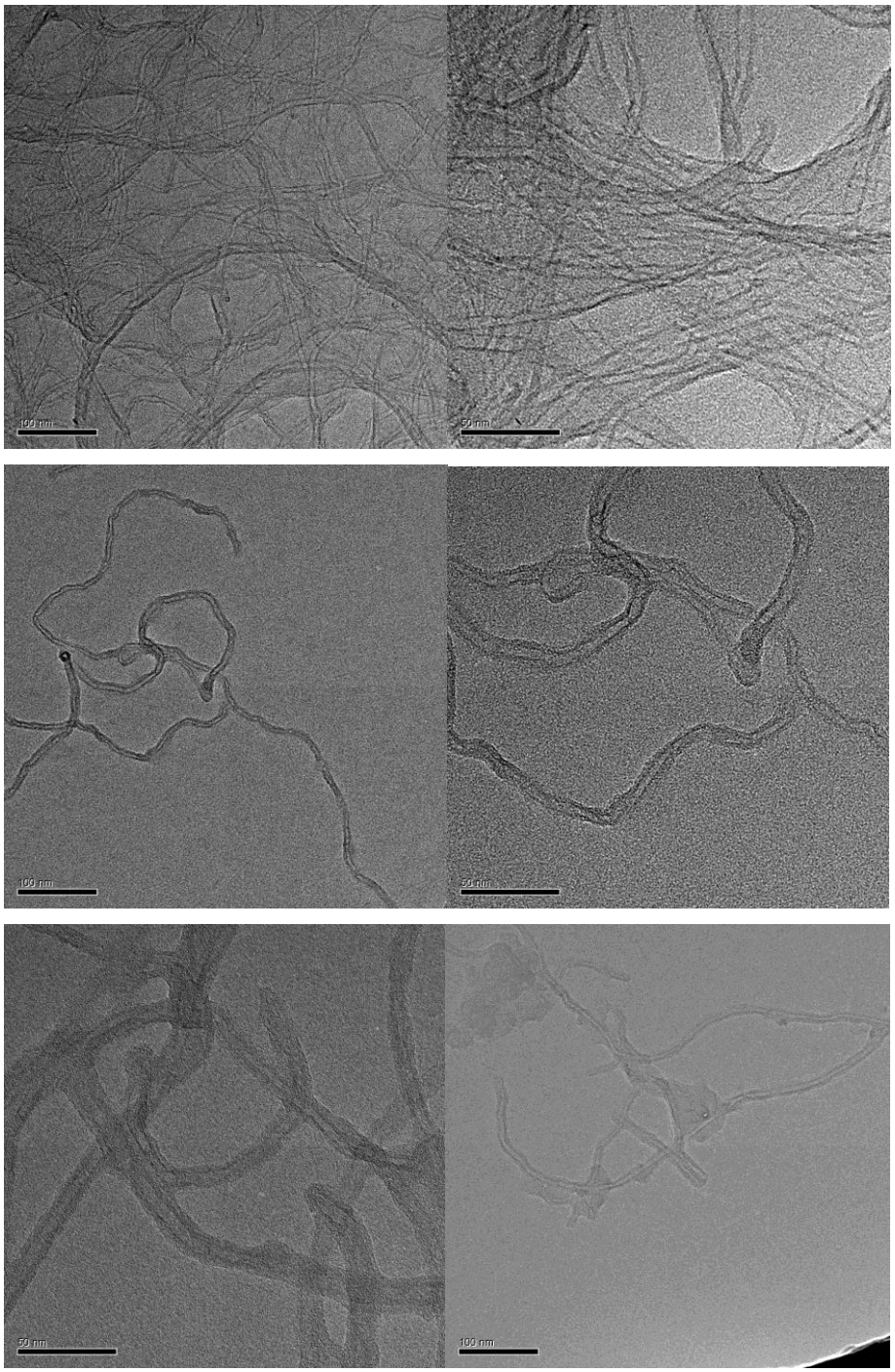

Figure 4. TEM images of water-dispersed pristine MWNT (top), **9-a** (middle), and **10-a** (bottom).

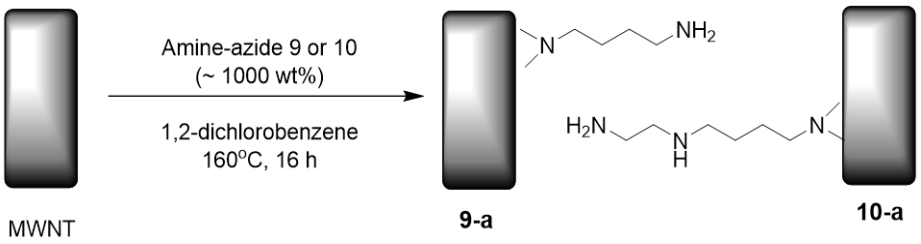

Scheme 8. Introduction of terminal amine group on MWNT surface.

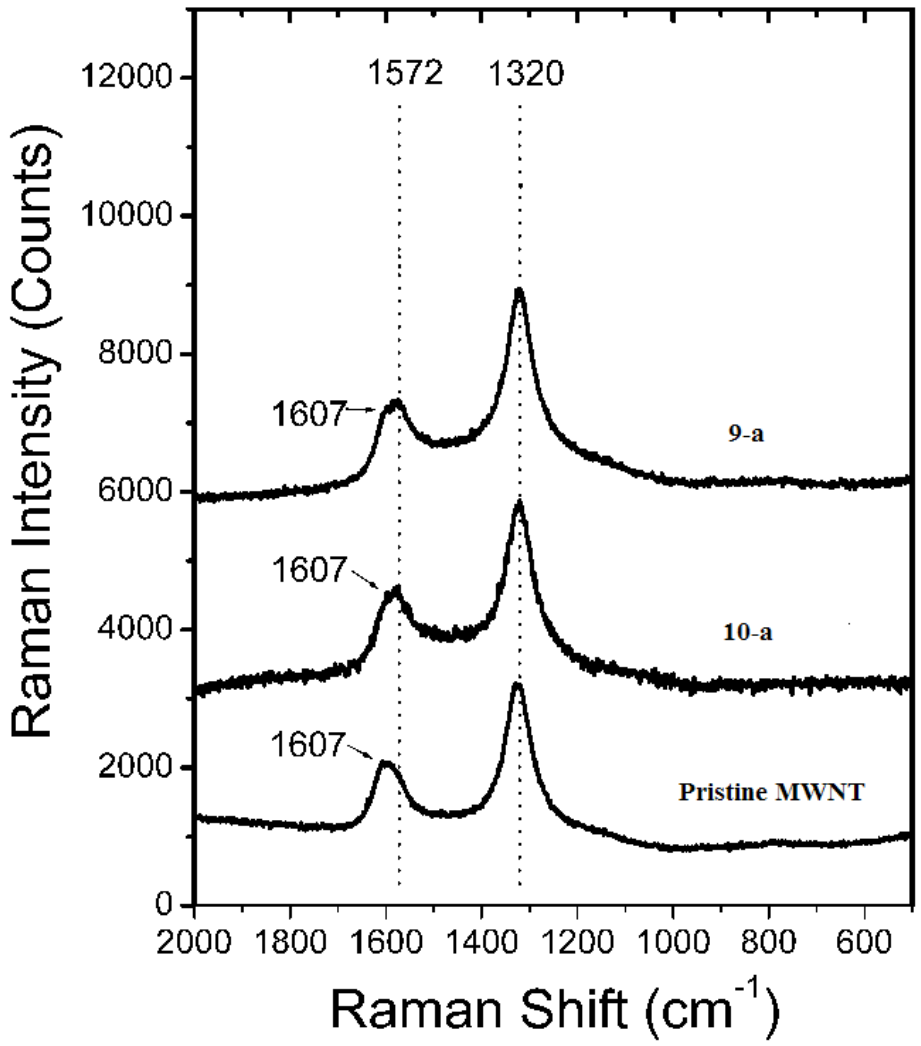

Figure 5.Raman spectra of pristine MWNT, **9-a**, and **10-a**.

Figure 5 shows Raman spectra of pristine MWNT, **9-a**, and **10-a**. In many experiments with SWNT, Raman spectrum could be used as a direct evidence for covalent sidewall functionalization. Pristine SWNT's exhibited a weak diameter-dependent radial breathing mode at ca. 230 cm^{-1} and a stronger tangential mode band (G-band) at ca. 1590 cm^{-1}. A weak band (D-band) centered at ca. 1290 cm^{-1} is attributed to sp^3-hybridized carbon in the hexagonal framework of the nanotube walls. This disorder mode band is enhanced, as expected, as groups are attached to the sidewalls of the nanotubes.[38] In other words, the increase of the D/G ratio means high degree of functionalization. But unike in the case of SWNT, pristine MWNT shows high intensity of D-band.[99] Therefore, it is hard to make a clear distinction of functionalized degree for MWNT (Figure 5) with D/G ratio in Raman spectra. Likewise, pristine MWNT, **9-a**, and **10-a** did not show much difference. There was a trivial shift of G-band (1607 -> 1572 cm-1) after the functionalization.

Although clear evidence was not found from the Raman spectra analyses, we relied on distinct changes in dispersibility of amine-functionalized MWNT (Amine-CNT) as a token for finctionalization. As a first application of amine-CNT, palladium salt was immobilized on amine-CNT surface using reduction with hydrogen gas. Due to high dispersibility of amine-CNT **9-a** in water, no surfactant was required for dispersion while palladium salt reduction (Scheme 9).

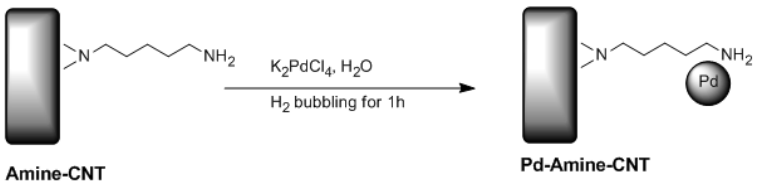

Scheme 9. Preparation of palladium loaded Amine-CNT upon reaction with K_2PdCl_2 in presence of H_2.

The Pd-amine-CNT was directly tested to a reaction for the verification of its catalytic activity. To our astonishment, with ICP-AES analysis we found that over 32 wt% of Pd-amine-CNT consisted of palladium metal. About 20 mg of Pd-amine-CNT (3.5 mol% of palladium) was used for Suzuki coupling. After the reaction was completed, the reaction mixture was transferred to a conical tube and the catalyst was recovered by centrifugation. Recovered catalyst was dried under vacuum and reused for the next reaction.

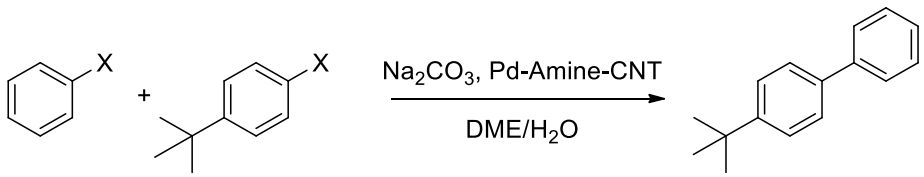

Scheme 10. Recycle test of Pd-Amine-CNT catalyst.

The Pd-amine-CNT catalyst showed catalytic activity in Suzuki coupling, but there is at least two obstacles for practical use of this catalyst. First, after the reaction, separation and recovery of the catalyst is troublesome. Second, leaching of the palladium catalyst is problematic. Actually, in the recycling test of the catalyst, significant loss of palladium species occurred during the extraction step. When the same reaction was carried out using aqueous phase of the first run's extracts, desired product was obtained in a quantitative yield.

Also, we tested hydrogenation reaction of phenyl acetylene by using 1 mol% of Pd catalyst. After reaction was complete, the catalyst was recovered by centrifugation and dried under vacuum oven and reused for recyling reaction. Result of recycling experiment is summarized in **Table 4**.

Table 4. Recycle test of Pd-amine-CNT.

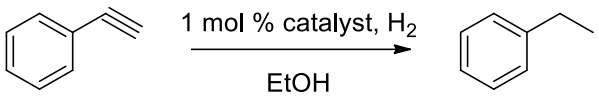

Run	1st	2nd	3rd	4th	5th	6th	7th
Time(min)	180	90	60	30	30	60	270
Conversion (%)	99	99	99	99	99	99	99

a. Yields were determined by GC analysis

At first reaction, Pd amine CNT showed excellent catalytic activity in hydrogenation. However, upon recycling, the catalytic activity of Pd amine CNT with Pd decreased due to leaching out of Pd. Also, we confirmed that the immobilization of palladium of the MWNT was not uniform through TEM (Figure 6).

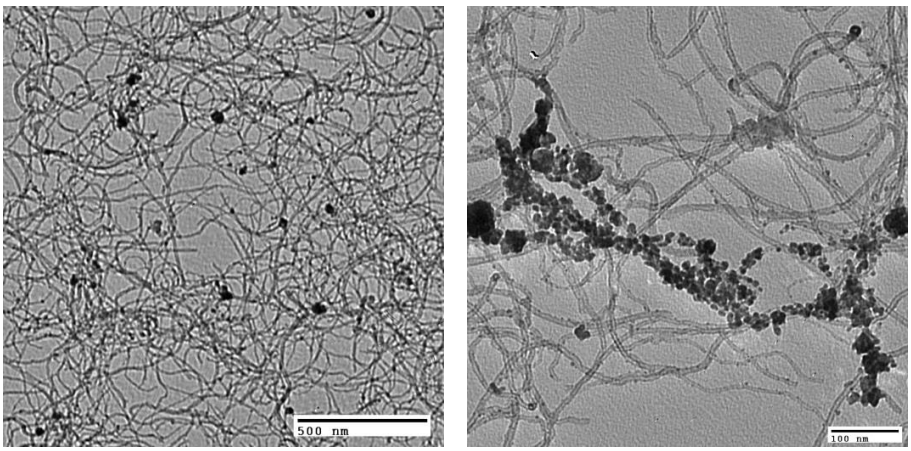

Figure 6. TEM images of Pd-amine-CNT with Pd

With these problems, to solve these problems, we decided to modify azido-linkers that have better ligating ability containing more oxygen or nitrogen to catch metal. Moreover, we introduced various reduction agents to load transition metals to immobilize uniformly on the surface of MWNT.

As mentioned earlier, we fixed palladium on the MWNT using hydrogen bubbling. Even though amine-CNT had enough palladium to make use of catalyst, palladium was loaded partially on MWNT and leached out after reaction. Then we tried to apply various reducing agents such as hydrogen gas and sodium borohydride to immobilize palladium**.**

The palladium loading with hydrogen gas or sodium borohydride resulted in metal on MWNT fixed irregularly as shown in TEM data. On the other hand, we introduced hydrazine monohydrate for immobilizing palladium, which allowed us to load palladium uniformly as shown in Figure 7 & Table 5.

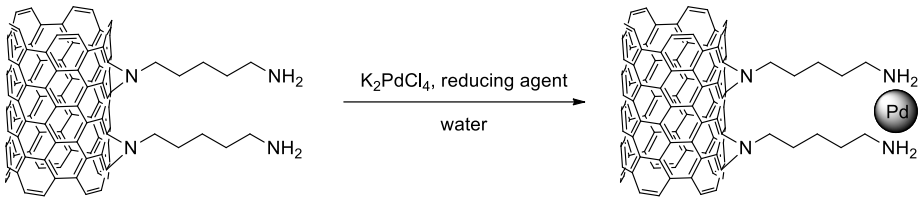

Scheme 11. Preparation of palladium loaded Amine-CNT upon reaction with K_2PdCl_2 in presence of several reducing agents.

a)

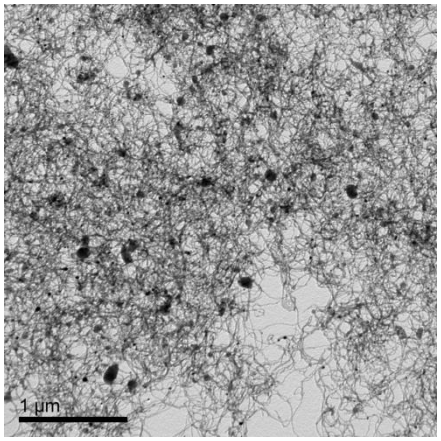

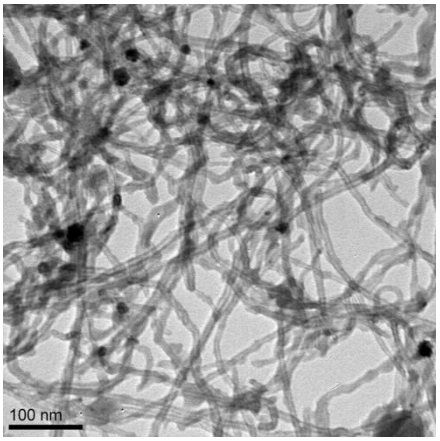

b)

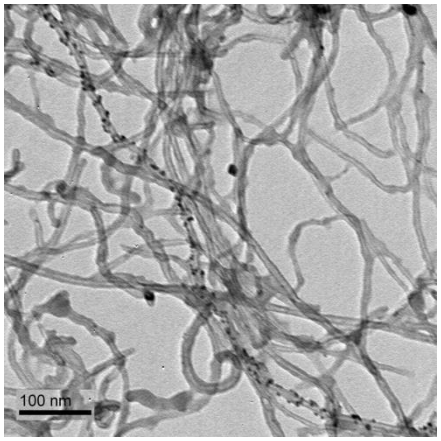

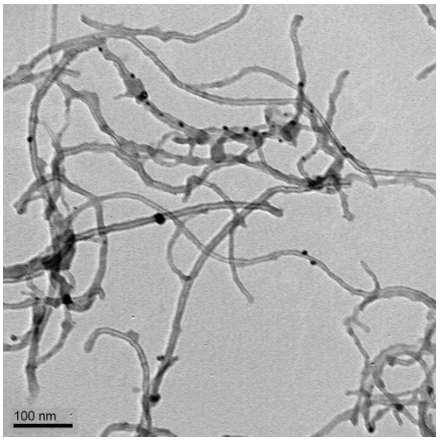

c)

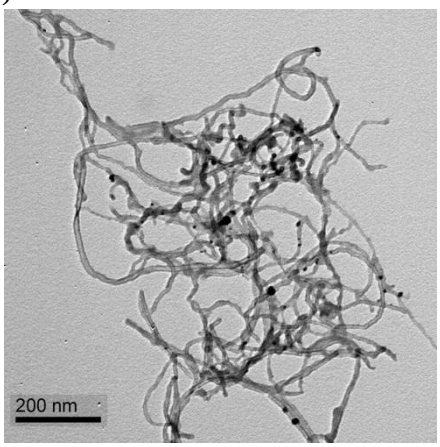

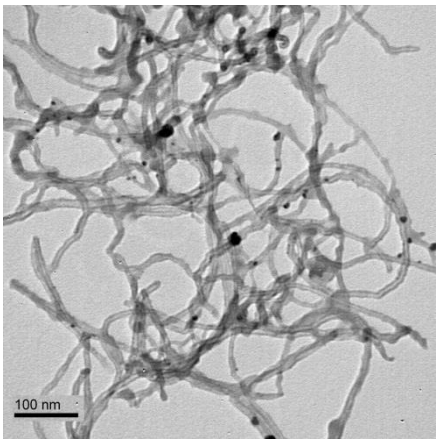

d)

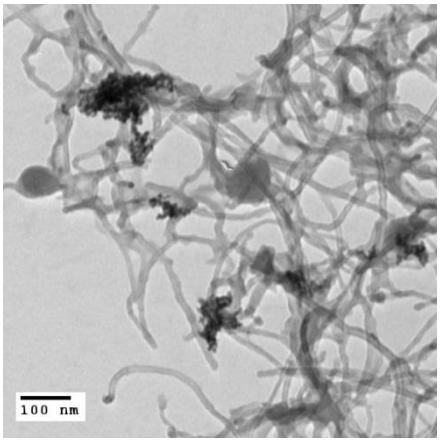

e)

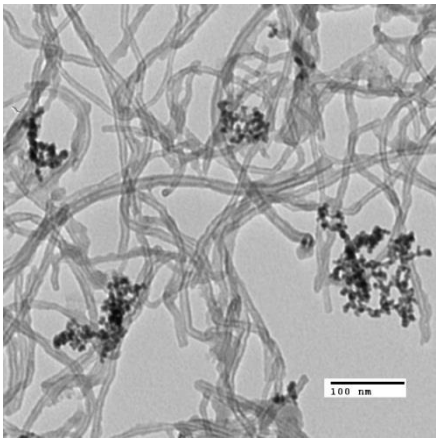

f)

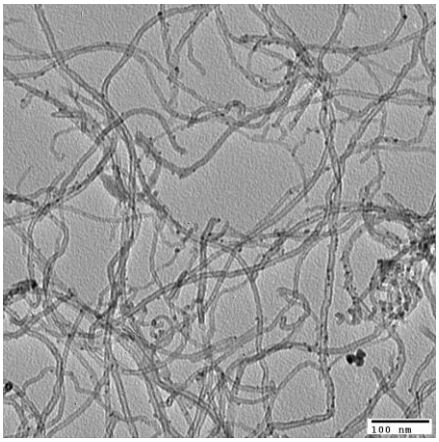

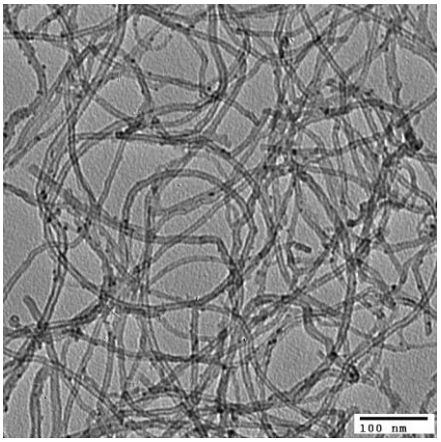

Figure 7. a) H_2 bubbling 30min, b) H_2 bubbling 1h, c) H_2 bubbling 2h, d) $NaBH_4$ 10wt%, e) $NaBH_4$ 25wt%, f) hydrazine monohydrate

Table 5. ICP data of Pd-amine-CNT

Pd	a	b	c	d	e	f
ICP data	9.78wt%	13.0wt%	6.38wt%	11.2wt%	10.2wt%	14.0wt%

Platinum has higher reduction potential than palladium, so it may require more powerful reducing agent. Shown in Figure 8 & Table 6, platinum with hydrogen gas was better loaded than using sodium borohydride.

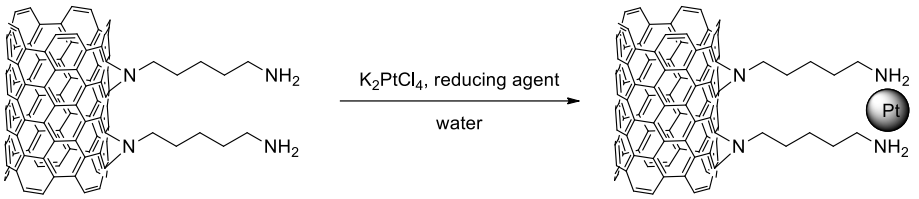

a)

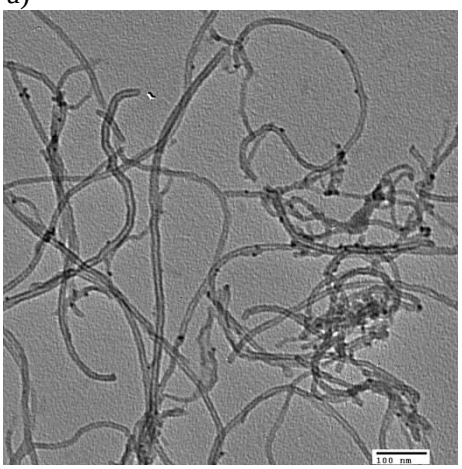

b)

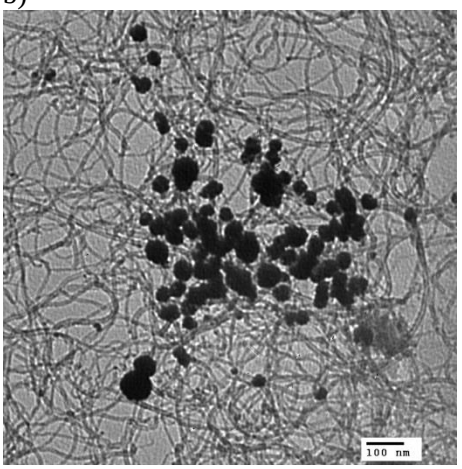

c)

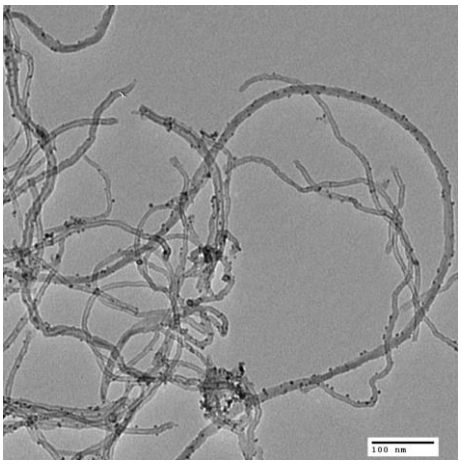

Table 6. ICP data of Pt-amine-CNT

	a	b	c
ICP data	5.25wt%	11.4wt%	12.4wt%

Figure 8. a) $NaBH_4$, b) salt adding after H_2 bubbling, c) H_2 bubbling after salt adding

Next, we modified the linker with pyridine moiety from Amine CNT as shown in scheme 12.[100]

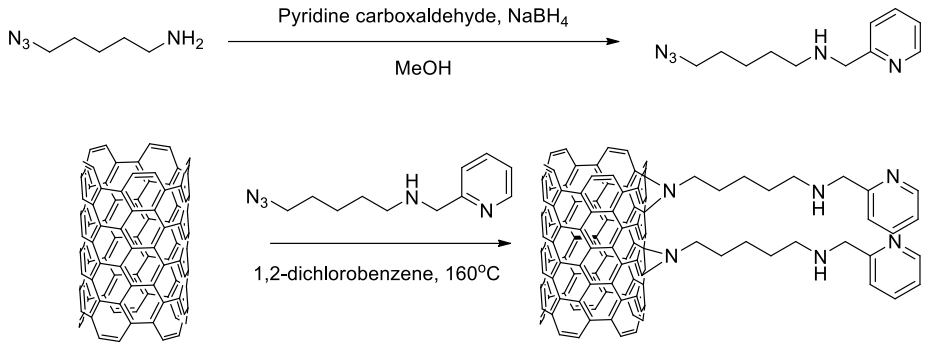

Scheme 12. Synthesis of the pyridine containing linker and functionalization of MWNT

Also, we designed the linkers with more heteroatoms such as nitrogen and oxygen to ensure tighter binding to metals (scheme 13).[101, 102]

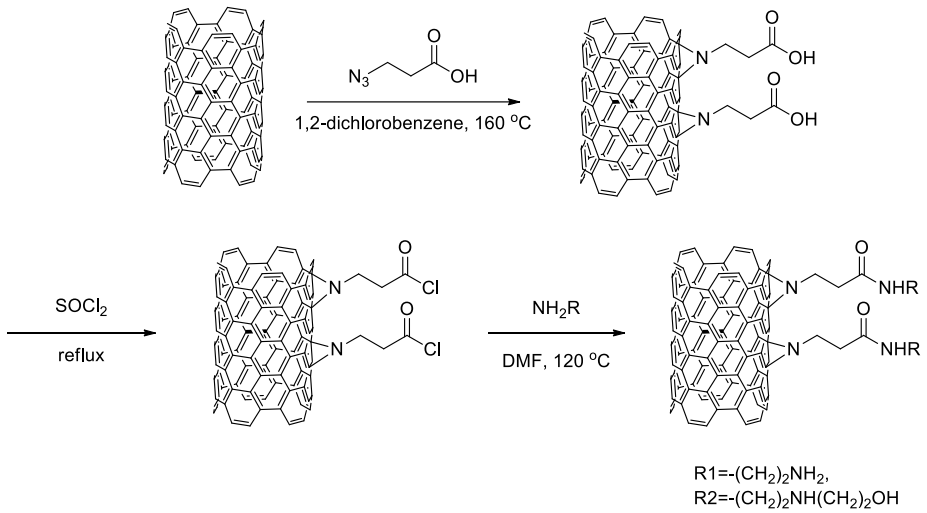

Scheme 13. Synthesis of functionalized CNT

We applied metal two different loading methods, palladium with hydrazine and platinum with hydrogen gas, into each MWNT with different linkers. Pyridine-containing linker with metal was not spread evenly, whereas regularly sized metals were ditstributed in R1 and R2 linker. And we carried out reduction of nitro gropus with these Pt-CNT-linkers. Even though pyridine linker CNT showed poor reactivity, we confirmed that platinium catalysts with R1 linker and R2 linker have good reactivity towards the nitro-reduction. After 10th recycle tests, These R2 linker catalytic systems showed the good distribution of metal on the functionalized MWNT to peform recycle experiments over 10 times. As a result, a Pd-CNT catalyst was prepared through the incorporation of a new ligand system (R2 linker system). And then, transition metals were incorporated on the linker-MWNT via reductive methods. After immobilization of palladium on CNT, its role as a catalyst for C-C bond coupling reaction (Suzuki reaction) was examined.

All experiments on CNTs were carried out using MWNTs prepared by a chemical vapor deposition (CVD) method. Functionalized CNT (CNT-ED-OH) was confirmed by Fourier-transform infrared (FTIR) spectrometry, elemental analysis (EA) and Thermal Gravimetric Analysis (TGA). Pd-CNT-ED-OH catalyst (Scheme 14) was prepared using various reducing agents. Detailed procedure and data are included in the experimental section.

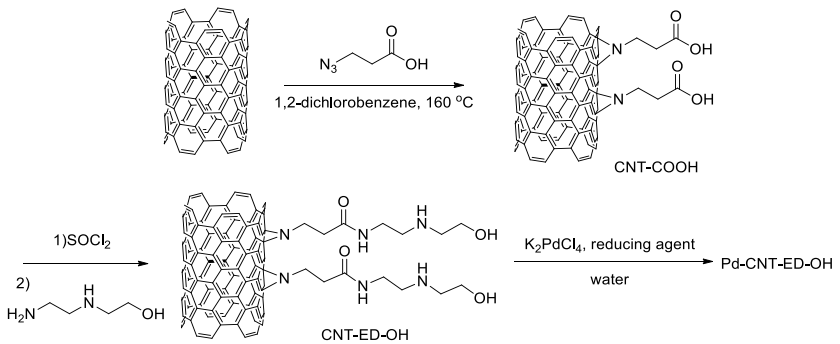

Scheme 14. Synthesis of Pd-CNT-ED-OH

The infrared spectrum of CNT-COCl (Figure 9-3) exhibited a peak at 1713 cm-1, indicative of the C=O stretching vibration of the COCl group. The C=O stretching frequency corresponding to the amide bond appeared at 1640 cm-1 (Figure 9-4). The band at 1384 cm−1 was assigned to the C-N bond stretch.

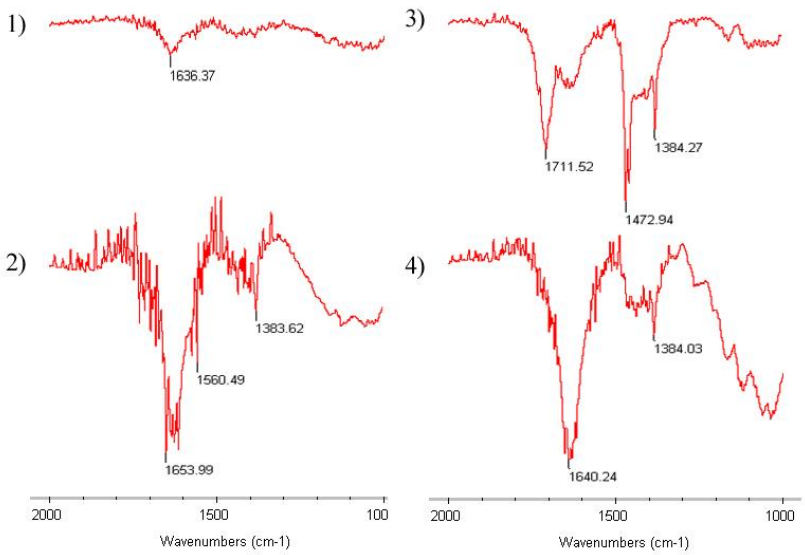

Figure 9. FT-IR of functionalized CNT 1) CNT-pristine, 2) CNT-COOH, 3) CNT-COCl, 4) CNT-ED-OH

The degree of functionalization on the MWNT could be calculated from the weight loss between 200 ^{o}C and 800 ^{o}C on TGA (Table 7). Comparison of the data from EA and TGA showed no significant differences, confirming successful installation of the linker. Palladium content in the synthesized catalyst was 0.98 wt% as measured by Inductively Coupled Plasma Mass Spectrometry (ICP-MS). The shape and size of the palladium nanoparticles on Pd-CNT-ED-OH could be assessed from the TEM image (Figure 10). Until now, a disadvantage of CNT catalysis has been the partial loading of palladium on MWNTs surfaces, with subsequent leaching of the metal after

reaction. We examined various reducing agents such as hydrogen gas, sodium borohydride and hydrazine, in an effort to efficiently immobilize palladium on the CNTs surface. Palladium loading with hydrogen gas and sodium borohydride resulted in irregularly fixed metal on MWNTs, as shown in the TEM data. Fortunately, use of the weaker reducing agent, hydrazine monohydrate for immobilization allowed uniform loading of palladium as shown in Figure 10. Further TEM images are supplied in the experimental section.

Table 7. Comparsion of TGA and Elemental analysis data

Sample	Weight loss between 200-480 ^{o}C (%)	The amount of functional groups per gram of MWNT (mmol)	Elemental (C,N,S) Analysis result (mmol)
CNT-COOH	34.78	6.20	4.00
CNT-ED-OH	30.96	1.66	1.80

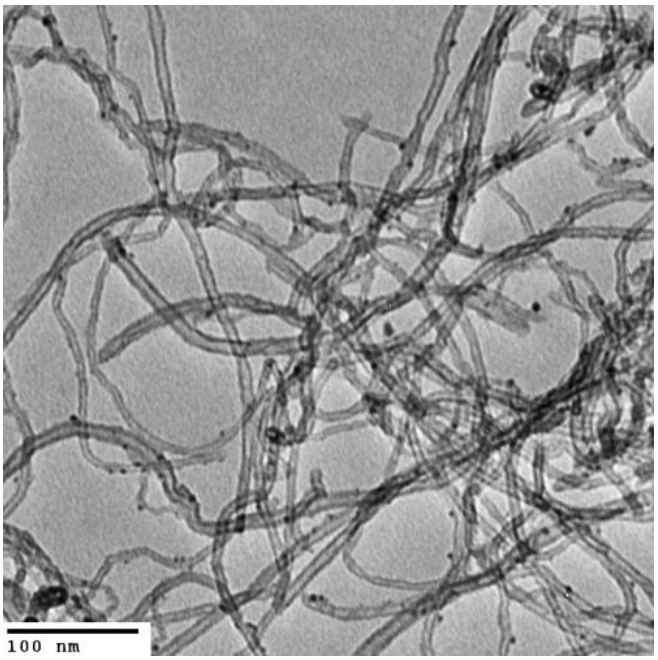

Figure 10. TEM image of Pd-CNT-ED-OH catalyst

The Pd-CNT-ED-OH catalyst was chosen for the reactivity test on the Suzuki reaction due to its excellent dispersion properties. A 25 mL two-necked reaction flask was charged with Pd-CNT-ED-OH catalyst (20 mg, 0.3 mol %) in degassed DMF (5.0 mL). Bromobenzene (52 µL, 0.50 mmol), phenylboronic acid (91 mg, 0.75 mmol), and anhydrous sodium carbonate (106 mg, 1.0 mmol) were added and the mixture was heated to 120 ℃. After 24 h, the reaction mixture was cooled to room temperature; solids formed during the reaction were collected by filtration. Pd-CNT-ED-OH was sequentially washed with DCM, water, and ethanol, and dried under vacuum for 2 h. Dried Pd-CNT-ED-OH was transferred to a 25-mL two-necked reaction flask, which was subsequently used for the next reaction cycle.

First, the catalytic activity of Pd-CNT-ED-OH in various solvents was tested for the Suzuki-coupling reaction of bromobenzene and phenylboronic acid. As shown in Table 8, the reaction in DME gave 47% yield based on GC measurement; in 1,4-dioxane, however, much lower yields were obtained (entries 1 and 2). Then a higher-boiling solvent, DMF, was investigated. As a result, the coupling reaction proceeded smoothly at 120 ℃ in DMF, yielding biphenyl in 60% yield upon the use of 10 mg (0.15 mol %) of Pd-CNT-ED-OH (entry 3). When a higher catalyst loading (20 mg, 0.3 mol %) of Pd-CNT-ED-OH was employed, excellent yield was observed (entry 4).

Table 8. Optimization of the Suzuki coupling reaction of phenyl boronic acid with bromobenzene[a]

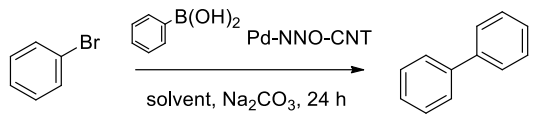

Entry	Pd-CNT-ED-OH amount (mg)	Solvent	Temperature (°C)	GC conversion (%)[b]
1	20	DME	80	47
2	20	1,4-Dioxane	80	4
3	10	DMF	120	60
4	20	DMF	120	90

[a] All reactions were carried out with 0.5 mmol bromobenzene in 5.0 mL of solvent with Pd-CNT catalyst. [b] Conversions were determined through GC analyses.

With the optimized reaction conditions in hand, we then carried out recycling tests on the Pd-CNT-ED-OH catalyst. After completion of the reaction, the catalyst was filtered off and the reaction products were directly analyzed with GC. The remaining catalyst was then washed with ethanol and water, dried under vacuum, and reused for the next reaction; the yields obtained for eight reaction cycles using the recycled catalyst are summarized in Table 9.

Table 9. Recycling Test of Pd-CNT-ED-OH catalyst of Suzuki reaction[a]

Run	Time (h)	GC yield (%)[b]
1	24 h	71
2		70
3		76
4		77
5		85
6		77
7		70
8		16

[a] All reactions were carried out with 0.5 mmol bromobenzene in 5.0 mL of solvent with 0.3 mol% of Pd-CNT-ED-OH catalyst. [b] Dodecane was used as an internal standard.

To examine the extent of Pd leaching from the CNT catalyst, the concentration of the CNT-bound palladium was measured through ICP-MS analysis. The palladium in the catalyst after seven reaction cycles was 0.70 wt%, corresponding to slight reduction from the initial concentration of 0.98 wt%. Figure 11 shows the TEM images of the Pd-CNT-ED-OH catalyst after the seventh run. Although a slight aggregation of nanoparticles was observed, the structure did not change significantly in size and shape.

We then carried out a series of Suzuki coupling reactions to test the scope of the substrates on the Pd-CNT-ED-OH catalyzed reaction (Table 10). The Pd-CNT-ED-OH catalyst showed a broad substrate scope for the reactions of various arylboronic acids with iodobenzene (entries 1–6). Under the optimized reaction conditions, a maximum yield of 94% could be obtained

(entries 1 and 2). Although the reactions of aryl bromides proceeded smoothly (entries 10–12), low yield was observed for the reaction of sterically hindered substrate (entry 12). Reaction of chlorobenzene (entry 13) gave a poor yield of the coupling product. The Pd-CNT-ED-OH catalyst also showed compatibility with various substituted aryl iodides in CNT-catalyzed reactions with phenylboronic acid, with moderate yields (entries 7–9).

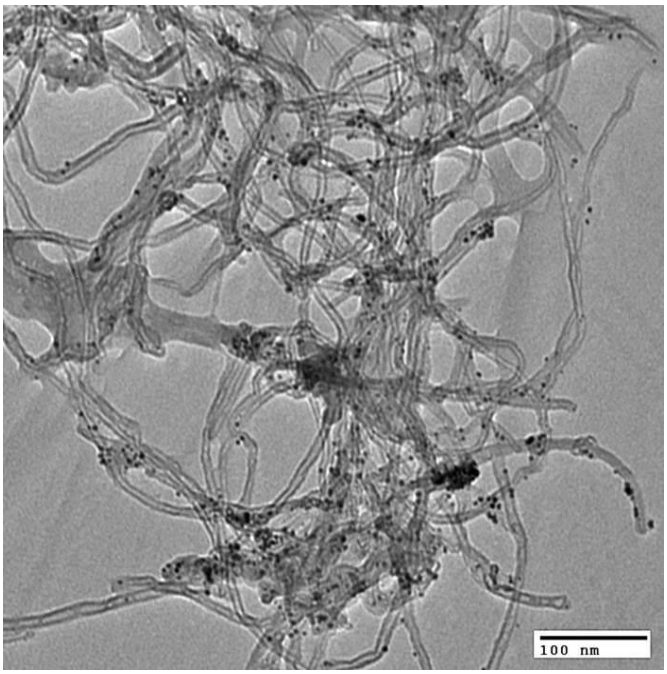

Figure 11. TEM image of Pd-CNT-ED-OH catalyst after seven reaction cycles.

Table 10. Substrate scope of Pd-CNT-ED-OH catalyzed Suzuki reaction[a]

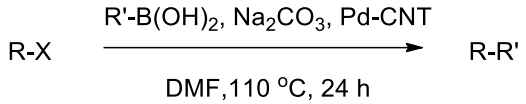

Entry	Aryl halide	Arylboronic acids	Yield(%)[b]
1		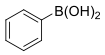	94[c]
2		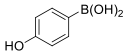	94
3		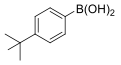	86
4		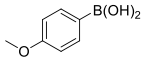	78
5		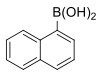	72
6		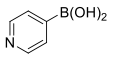	47
7			30
8			65
9	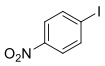		50
10	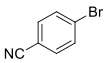	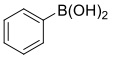	88
11	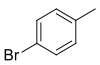		60
12			20
13			7[c]

[a] All reactions were carried out with 0.5 mmol aryl halide in 5.0 mL of solvent with 0.3 mol% of Pd-CNT-ED-OH catalyst [b] Isolated yield [c] Yields were determined through GC analyses

From our continuing study of the functionalized CNT and Pd-CNT, We focused on that carbon nanotube electron systems, suitable metal nanoparticle supporter for redox reactions. Therefore we synthesized Pd-Pt bimetallic nanoparticle catalysts using functionalized multi-wall carbon-nanotubes. We carried out reduction of nitro compounds using Pd-Pt CNT.

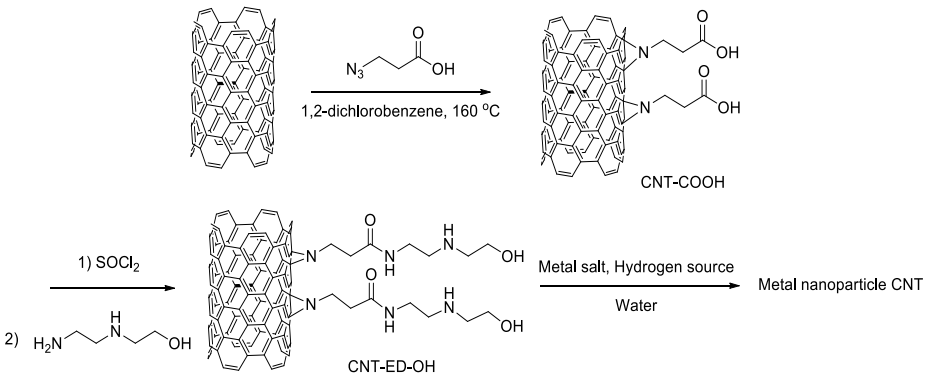

Scheme 15. Synthesis of Pd-Pt CNT

The Energy Dispersive Spectrometer (EDS) data indicate that metal and C are the major elements in the composite. Inductively coupled plasma (ICP) mass data of Pd and Pt concentrations in the Pd-Pt-CNT catalyst (Figure 12) were found to be 3.44 wt% (Pd) and 5.46 wt% (Pt). From the EDS results (Figure 13), we found that the atom ratio of Pd and Pt in Pd-Pt CNT is 1.25:1.16. Figure 1 shows the TEM images of the Pd-Pt-CNT. We confirmed that the nanoparticles of a uniform size (9~10 nm) are evenly distributed. More TEM images and EDS data are given in the experimental section.

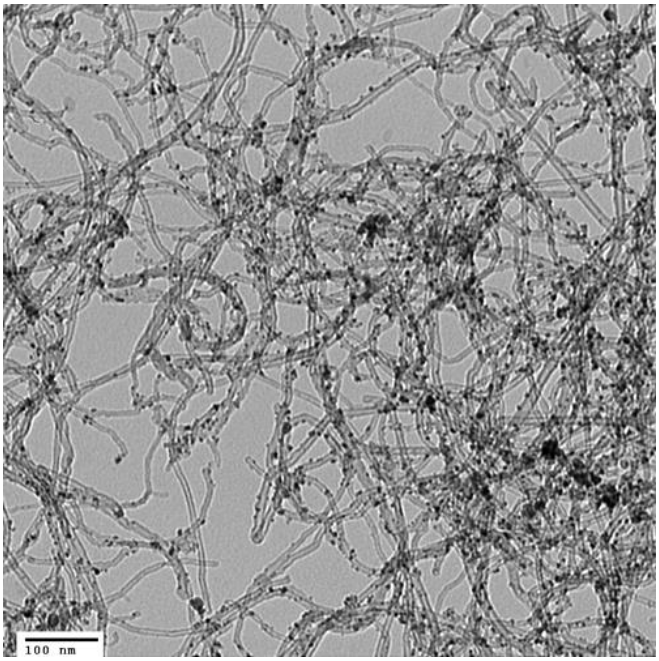

Figure 12 TEM images of Pd-Pt CNT

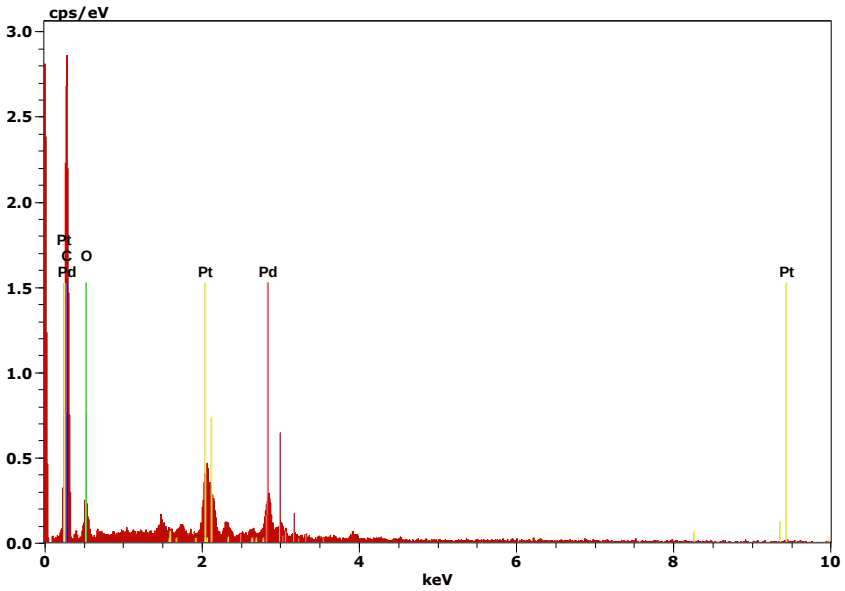

Figure 13 EDS spectrum of Pd-Pt CNT

Pd-Pt-CNT catalyst (10 mg) in degassed EtOH (4 mL) was placed in a 25-mL two-necked round-bottom flask. Nitrobenzene (52 μL, 0.5 mmol) was added to the mixture under H2 (1 atm) and the mixture was stirred at ambient temperature. After completion of the reaction, the mixture was filtered. Pd-Pt CNT filtrate was washed with dichloromethane and ethanol, and then dried under vacuum for 2 h to be used in the next reaction. Other substrates have been examined under the same reaction conditions.

First, the catalytic activity of the Pd-Pt-CNT was tested for the reduction of nitrobenzene to aniline under various conditions as seen in Table 1. We evaluated the catalytic activity of metals (Pd, Pt) separately using 1 mol% (based on Pd) metal-supported CNT. When the reaction was conducted using Pd-CNT, full conversion was observed after 1 h; with Pt-CNT catalyst in 2 h (Table 11, entries 1 and 2, respectively). However, when bimetallic Pd-Pt-CNT was used as a catalyst, the reaction was complete in 20 min without any trace of side products such as nitroso- or N-hydroxylaminobenzene (entry 3). This result shows that the bimetallic system has a synergistic effect in the nitro reduction. When the reaction was performed in various solvents such as THF, DME, dichloromethane, and water (entries 4-7), the reactivity was the highest in ethanol, though there were no apparent differences in dispersibility of the catalyst.

Table 11. Optimization of nitrobenzene reduction conditions [a]

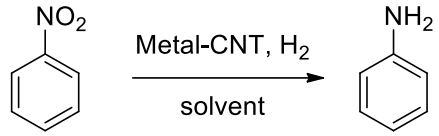

Entry	Catalyst	Solvent	Time (min)	GC conversion(%)[b]
1	Pd-CNT	EtOH	60	99
2	Pt-CNT	EtOH	120	99
3	Pd-Pt-CNT	EtOH	20	99
4	Pd-Pt-CNT	THF	30	53
5	Pd-Pt-CNT	DME	30	51
6	Pd-Pt-CNT	DCM	30	83
7	Pd-Pt-CNT	Water	30	15

[a] Reaction conditions: 0.5 mmol of nitro compound, hydrogen gas (balloon 1 atm), 4.0 mL of ethanol with 1 mol% of metal-CNT catalyst at ambient temperature. [b] All the conversions were determined by GC analysis

With the optimized reaction conditions in hand, we carried out recycling reactions using the Pd-Pt-CNT catalyst (Table 12). After the reaction was complete, the catalyst was collected by filtration; washed with ethanol, water, and DCM; and reused for the next reaction. The results are summarized in Table 2. The catalyst showed consistently high activity through the 10th reaction. The 11th reaction was slightly slower (30 min). To examine if metal nanoparticles from the CNT catalyst leached, the catalyst systems were analyzed for metals through ICP analysis. The Pd and Pt contents in the catalyst after 11 reaction cycles were 3.13 and 4.88 wt%, respectively, slight decreases from the original 3.44 and 5.46 wt%. Figure 12 shows the TEM image of the catalyst after the 11th run, where the nanoparticles appear somewhat aggregated.

Table 12. Recycling test of Pd-Pt CNT catalyst in nitrobenzene reductions[a]

Run	Time(min)	GC yield(%)[b]
1	20	99
3	20	99
5	20	99
7	20	99
9	20	99
10	20	99
11	30	99

[a] Reaction conditions: 0.5 mmol of nitro compound, H_2 balloon, 4.0 mL of ethanol with 1 mol% of metal-CNT catalyst at ambient temperature. [b] Anisole was used as an internal standard.

To examine the substrate scope of the Pd-Pt-CNT-catalyzed reduction, we tested reactions of various substrates under the optimized conditions shown in Table 11. Table 13 shows that the Pd-Pt-CNT catalyst showed excellent activity on a variety of substrates. In particular, other reducible functional groups such as benzyl, ester, ketone and halogen groups (entries 4-5, and 10-12) were not reduced at all. Reduction of 2,6-dinitrotoluene was complete in 1 h (entry 6). In addition, the substrates containing electron-withdrawing amide (entry 8), acetyl (entry 10), and halogen groups (entries 11-12) also showed good reactivity. Though the reduction of an aliphatic nitro compound took longer than that for nitroarene compounds, excellent yield of the desired products was obtained (entry 13). Olefin reductions were also carried out with the optimized conditions obtained in the nitro reduction. The Pd-Pt-CNT catalyst showed exceedingly good catalytic efficiency as shown in Table 14. The reduction of styrene proceeded extremely well and was complete in 30 min (entry 1). The reduction of di- or tri-substituted cyclic olefins produced excellent yields (entries 2-3). Sterically hindered and 1,1-disubstituted olefins were also reduced smoothly (entries 2, 5 and 4, respectively). Allylic alcohol was also reduced cleanly to the corresponding alkanol (entry 6). The slow reaction of trans-stilbene (entry 7) may be due to the low solubility of trans-

stilbene; the reaction was complete in 20 h at ambient temperature. Reduction of an alkyl-substituted olefin also gave good conversion (entry 8). These results clearly show that the Pd–Pt-CNT catalyst has remarkably high activity for the reduction of a variety of nitro compounds and olefins.

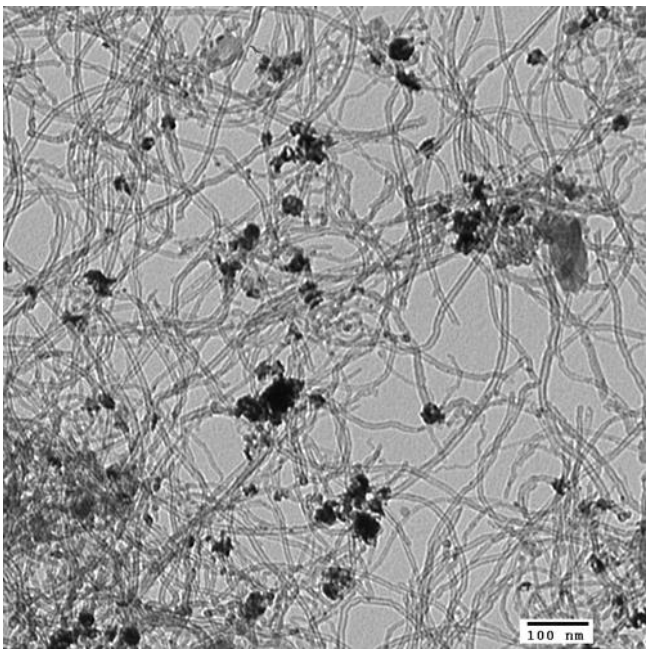

Figure 12. TEM images of Pd-Pt CNT after 11 times of use

Table 13. Substrate scope of Pd-Pt CNT catalyzed nitro group reductions.[a]

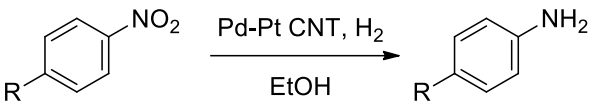

Entry	Substrate	Product	Time (h)	Yield(%)[b]
1	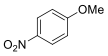	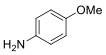	0.5	95
2	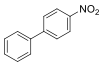	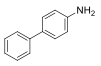	1	99
3		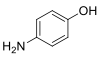	0.5	98
4	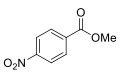	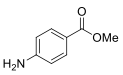	0.5	97
5	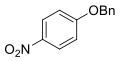	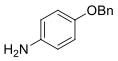	1	99
6			1	99
7	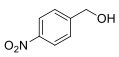	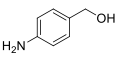	1	93
8	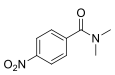	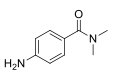	0.5	94
9	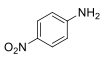	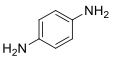	0.5	87
10	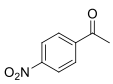	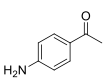	0.5	97
11			1	99[c]
12		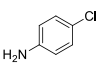	1	99[c]
13	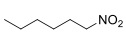	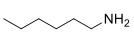	3	98[c]

[a] Reaction conditions: 0.5 mmol of nitro compound, hydrogen gas(balloon 1 atm), 4.0 mL of ethanol with 1 mol% of metal-CNT catalyst at ambient temperature. [b] Yields of isolated products. [c] Yields were determined by GC analysis using anisole as an internal standard

Table 14. Substrate scope of Pd-Pt CNT catalyzed olefin group reductions.[a]

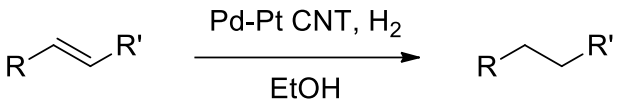

Entry	Substrate	Product	Time (h)	Yield (%)[b]
1			0.5	99[c]
2			0.5	99[c]
3			4	99
4			1.5	98
5			2	94
6	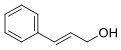	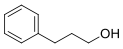	2	99
7	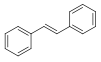	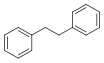	20	96
8	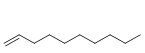		1	99[c]

[a] Reaction conditions: 0.5 mmol of olefin compound, H2 balloon, 4.0 mL of ethanol with 1 mol% of metal-CNT catalyst at ambient temperature. [b] Yields of isolated products unless otherwise noted. [c] Determined by GC analysis using anisole as an internal standard.

III. Conclusion

The synthesis and characterization of MWNTs modified by surface functionalization using nitrene chemistry and the utility of the resulting material as a new support for Pd catalysts were reported. Various reduction methods were scanned to immobilize Pd on the MWNT surfaces and use of hydrazine hydrate was found to be the most optimal. These new catalytic systems exhibited good distribution of the metal on the functionalized MWNT. The new Pd-MWNT catalyst showed good reactivity in Suzuki coupling reactions. To new linkers incorporating N-(2-hydroxyethyl) ethylene diamine were effective in holding the metal more effectively than simple amine linkers. As a result, the catalyst was recycled over seven reactions before any loss of catalytic activity was observed, with only minimal catalyst loading (0.3 mol %). To develop more effective CNT-based transition metal catalysts, we are examining additional organic reactions in which these catalytic systems can be applied. Therefore we synthesized new Pd-Pt bimetallic nanoparticle catalysts system. We have shown that efficient reductions of nitro compounds and alkenes can be achieved using Pd-Pt bimetallic nanoparticle CNT catalysts with H_2 at ambient temperature in ethanol. With the optimized conditions, nitrobenzene was converted to aniline in 99% yield in 20 min and various nitro compounds and alkenes were cleanly reduced. Furthermore, using this bimetallic catalyst, compounds containing other reducible functionalities were converted to their corresponding products with excellent chemoselectivities. In addition, the catalyst was recycled 10 times without any loss of activity. Therefore, the Pd-Pt bimetallic nanoparticle catalysts on MWNTs form an efficient catalytic reaction system and are air- and moisture-stable, without producing any hazardous waste.

IV. Experimental

General

All our works on CNTs were carried out using multi-wall nanotubes (MWNT) prepared by chemical vapour deposition (CVD) method. All the reactions were performed by using oven-dried glassware and all commercial materials were used without purification. Sonication was performed in a 120 W ultrasonic bath (Branson, B-3210) and Sonics & Vibra cell VCX 750. GC analyses were performed with a HP-6890 series with a HP-5 capillary column (30 m x 0.25 mm; coating thickness 0.25 μm). TGA was performed on a TGA Q5000 V3.10 Build 258 instrument at a heating rate of 10 °C min^{-1} under a nitrogen flow. Elemental (C, H, N) analysis was done on a Flash EA 1112. Loading metal quantification was measured by inductively coupled plasma (ICP) mass spectrometry on a Varian 820-MS. TEM was performed at 100 kV on a Hitachi H-7600 electron microscope. The TEM sample was dispersed in anhydrous ethanol and spread onto 300 mesh Cu grids. EDS was measured conducted using a field emission scanning electron microscope, SUPRA 55VP.

Representative procedure of diazotization using MWNT

To a oven-dried 500 mL beaker, 60 mg of MWNT was charged then dispersed in 50 mL of 1,2-dichlorobenzene. The dispersion was sonicated with tip sonicator for 10 min then transferred to 250 mL two-necked rbf. Then 4-nitroanilne (2.76 g) solution in 25 mL of acetonitrile was added to rbf. The reaction mixture was bubbled with argon gas for 15 min. Then 2.86 mL of isoamyl nitrite was added at once to the resulted mixture at 60°C. After 4 days, the reaction mixture was poured into 200 mL of dichloromethane. The suspension was filtered through aBuchner funnel and washed with DCM,

THF, and ether. Gathered black-colored flat disk was dried in vacuum oven at 65ºC for 18 h.

Preparation of linkers

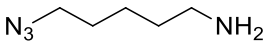

Sodium azide (2.54 g, 39.1 mmol) was added to dibromopentane (3.00 g 13.1 mmol) in 65.2 mL of dimethylforamide (DMF). After water (6.52 mL) was added, mixture was heated at 80 ºC and stirred overnight. The resulting solution was concentrated *in vacuo* for the removal of DMF. The mixture was mixed with water and extracted with dichloromethane (3 x 65 mL). Combined organic layers were dried over sodium sulfate, filtered, and concentrated under reduced pressure. Diazidopentnae (1.75 g, 11.4 mmol, 87.0% yield) was obtanied.

Diazidopentane (1.75 g, 11.4 mmol) was soluted in 37.8 mL of ether and 37.8 mL of 2N HCl. Triphenyl phosphine (2.83 g, 10.8 mmol) in 37.8 mL of ethyl acetate was added slowly at 0 ºC. After stirring at room temperature for 12 h, the reaction mixture was concentrated *in vacuo* for the removal of ether and ethyl acetate. The mixture was extracted with dichloromethane (3 x 40 mL). Sodium bicarbonate solution was added into water layer at 0 ºC until pH 9. The reaction mixture was extracted with ethyl acetate (3 x 60 mL). Combined organic layers were dried over sodium sulfate, filtered, and concentrated under reduced pressure. Product (1.03 g, 8.13 mmol, 71.3% yield) was obtained.

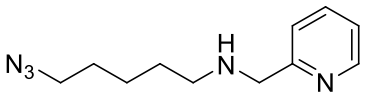

To a solution of 2-pyridine carboxaldehyde (0.819 g, 7.60 mmol) and 5-azidopentylamine (1.00 g, 7.80 mmol) in 26.0 mL of methanol was added sodium borohydride (295 mg, 7.8 mmol) slowly at 0 ^{o}C. Then, the mixture was warmed up to room temperature and stirred overnight. Water (26.0 mL) was added to the mixture and methanol was removed by evaporation. Aqueous layer was then extracted with ethyl acetate (3 x 30 mL) and the combined extracts were dried over $MgSO_4$. After concentration, the residue was purified by chromatography on silica gel to give brownish oil (1.42 g, 6.51 mmol, 83.4% yield).

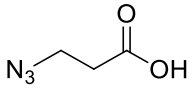

3-bromopropionic acid (3.00 g, 19.6 mmol) was dissolved in acetonitrile (31.6 mL) and sodium azide (2.57 g, 39.5 mmol) was added to the solution, the mixture was refluxed for 4 h. Acetonitrile was removed *in vacuo* and the resulting residue was suspended in 32 mL of ethyl acetate and extracted with 0.1 N HCl (2 x 30 mL), water (2 x 30 mL) and brine (2 x 30 mL). The organic layer was dried with sodium sulfate to afford 3-azidopropionic acid (1.98 g, 17.2 mmol) in 87.0% yield.

Preparation of amine-CNT using nitrene chemistry

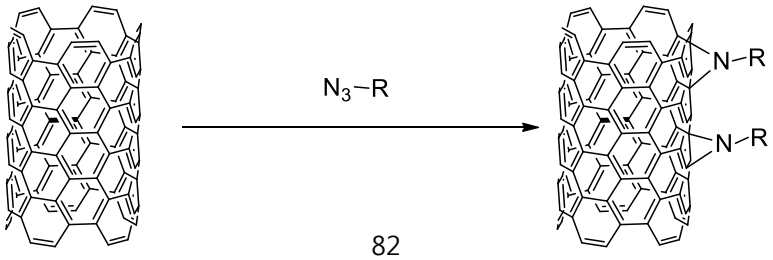

An oven-dried 500 mL beaker was charged with 100 mg of MWNTs, and then it was dispersed in 200 mL of 1,2 -dichlorobenzene. The mixture was sonicated with an ultrasonicator apparatus for 60 min (20 min x 3), transferred to 500 mL two-necked flask, bubbled with argon gas for 10 min and then heated to 160 ^{o}C. After 30 min, 3-azidopropanoic acid (1.00 g) was dissolved in 10 mL of 1,2-dichlorobenzene, and slowly added to the MWNTs dispersion (4 mL/h). The reaction mixture was stirred at 160 ^{o}C for 16 h, then cooled to room temperature, and poured into 200 mL of THF. A black CNT-carboxylate (CNT-COOH) material was obtained by filtration, washing, and drying in a vacuum oven. Next, to an oven-dried 250 mL reaction flask, was added 100 mg of CNT-COOH dispersed in 20 mL of thionyl chloride, which was sonicated for 1 h. After sonication, the mixture was bubbled with argon for 10 min, and then refluxed overnight. Thionyl chloride was removed through evaporation. To the residue was added 200 mL of DMF followed by sonication of the mixture for 1 h and stirring at 120 ^{o}C. After 10 min, 1 mL of N-(2-hydroxyethyl) ethylenediamine was slowly added with stirring at 120 ^{o}C (Scheme 1). After 12 h, the mixture was cooled to room temperature, filtered, washed with water and THF, and dried in a vacuum oven at 70 ^{o}C for 12 h.

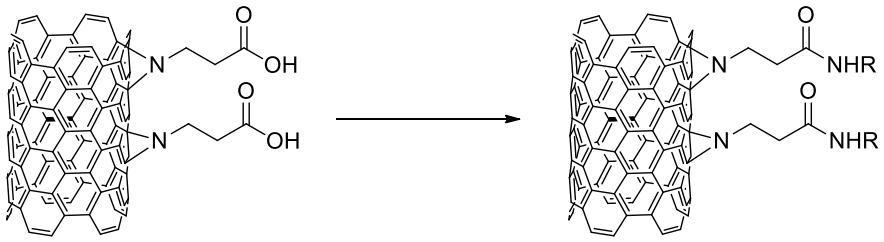

R=-$(CH_2)_2NH_2$,
R=-$(CH_2)_2NH(CH_2)_2OH$

Preparation of Pd-CNT-ED-OH with hydrogen gas bubbling

To an oven-dried 500 mL beaker, 100 mg of functionalized CNT (CNT-ED-OH) was dispersed in 200 mL of distilled water, then sonicated with tip sonicator for 60 min (20 min x 3). The dispersion was transferred to 500 mL two-necked reaction flask, then K_2PdCl_4 (50 mg) dissolved in 10 mL water was slowly added into reaction flask. The reaction mixture was bubbled with hydrogen gas. The resulting mixture was allowed to stir under hydrogen gas (1 atm) for another 12 h. The mixture was poured into 200 mL of THF. Black precipitate was gathered by filtration and then was washed with water and THF, and then dried in vacuum oven at 70 ^oC for 12 h.

Preparation of Pd- CNT-ED-OH with sodium borohydride

To an oven-dried 500 mL beaker, 100 mg of functionalized CNT (CNT-ED-OH) was dispersed in 200 mL of distilled water, then sonicated with tip sonicator for 60 min (20 min x 3). The dispersion was transferred to 500 mL two-necked reaction flask, then K_2PdCl_4 (50 mg) dissolved in 10 mL water was slowly added into reaction flask. The reaction mixture was bubbled with argon gas for 10min, then 10 mL of aqueous sodium borohydride solution was slowly added (4 mL/h) and the mixture was stirred under argon gas (1 atm) for another 12 h. The mixture was poured into 200 mL of THF. Black precipitate was gathered by filtration and then was washed with water and THF, and then dried in vacuum oven at 70 ^oC for 12 h.

Preparation of Pd-CNT-ED-OH with hydrazine monohydrate

To an oven-dried 500 mL beaker, 100 mg of functionalized CNT (CNT-ED-OH) was dispersed in 200 mL of distilled water, then sonicated with tip sonicator for 60 min (20 min x 3). The dispersion was transferred to 500 mL two-necked reaction flask and bubbled with argon gas for 10 min, then

K_2PdCl_4 (50 mg) dissolved in 10 mL water was slowly added into reaction flask. The reaction mixture was bubbled with argon gas for 10 min again and heated to 80 oC. After 10min, 10 mL of hydrazine monohydrate was slowly added (4 mL/h) and the mixture was stirred under argon gas (1 atm) for another 12 h. The mixture was poured into 200 mL of THF. Black precipitate was gathered by filtration, washed with water and THF, and then dried in vacuum oven at 70 ^oC for 12 h.

TGA curve of CNT–COOH and CNT-ED-OH

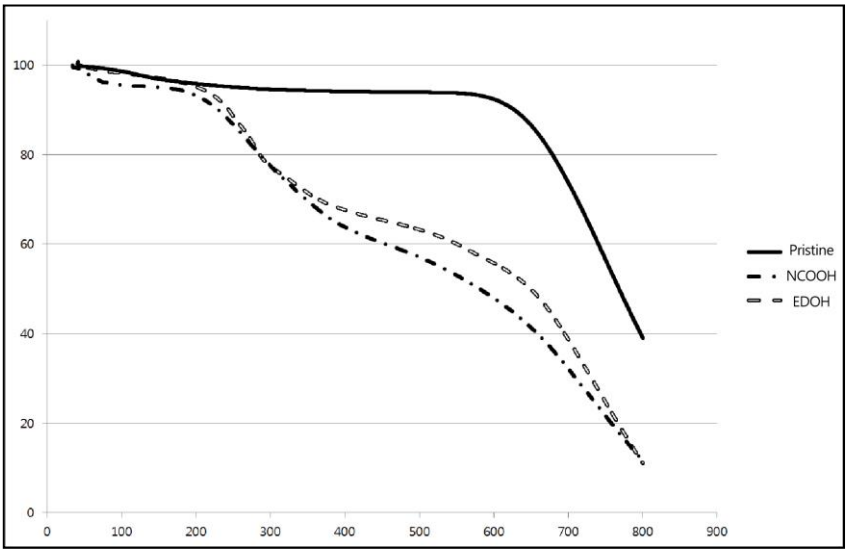

Optimization of the Suzuki coupling reaction of phenyl boronic acid with bromobenzene. [a,b]

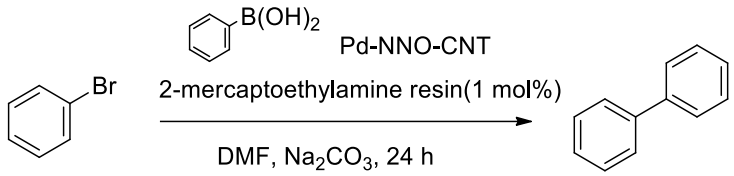

[a] All reactions were carried out with 0.5 mmol bromobenzene in 5.0 mL of solvent with Pd-CNT catalyst (0.3 mol%). [b] Conversions were determined through GC analyses.

Investigation on leaching of Pd from the Pd-CNT-ED-OH catalyst system.

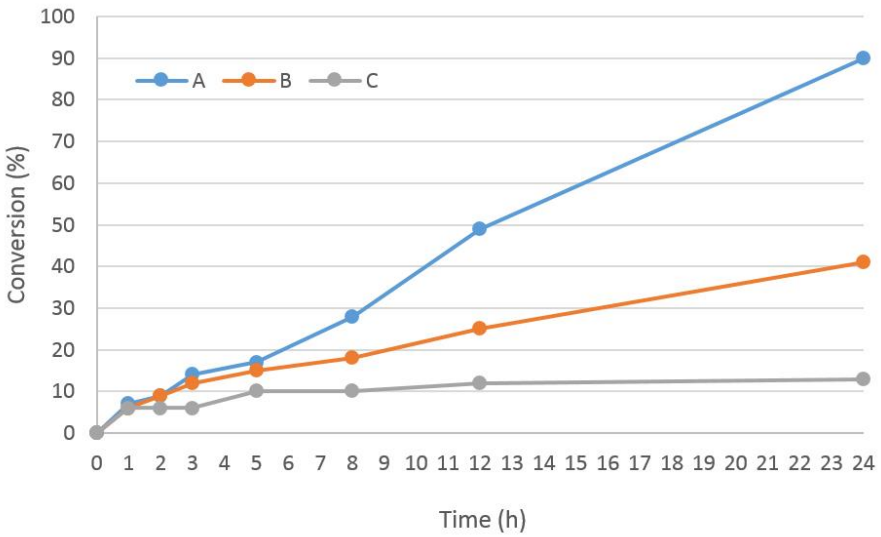

[A] Progress of the Suzuki reaction using the Pd-CNT-ED-OH catalyst. [B] Progress of the Suzuki reaction after addition of 2-mercaptoethylamine resin at 5 h. [C] Progress of the Suzuki reaction when 2-mercaptoethylamine resin was added at the beginning togeher with the Pd-CNT-ED-OH catalyst.

Preparation of bimetallic nanoparticle CNT

Pd-CNT: In an oven-dried 500-mL beaker, 100 mg of MWNT was dispersed in 200 mL of distilled water, and then the mixture was sonicated with a tip sonicator for 60 min (20 min ×x 3). The dispersion was transferred to a 500-mL two-necked reaction flask and then bubbled with argon gas for 10 min. K_2PdCl_4 (50 mg) was dissolved in 10 mL water, and then added slowly into the reaction flask. The reaction mixture was again bubbled with argon gas for 10 min and heated 80 ℃, after which 10 mL of hydrazine monohydrate was slowly added (4 mL/h) and the mixture was stirred under argon gas (1 atm) for another 12 h. The mixture was poured into 200 mL of THF. Black precipitate (Pd-CNT) was gathered by filtration, and it was washed with water and THF, and then dried in a vacuum oven at 70 ℃ for 12 h.

Pt-CNT: In an oven-dried 500-mL beaker, 100 mg of MWNT was dispersed in 200 mL of distilled water. It was then sonicated with a tip sonicator for 60 min (20 min ×x 3). The dispersion was transferred to a 500-mL two-necked reaction flask, K_2PtCl_4 (50 mg) was dissolved in 10 mL water, and then slowly added into the reaction flask. Hydrogen gas was bubbled through the reaction mixture for 1 h. The resulting mixture was stirred under hydrogen gas (1 atm) for another 12 h. The mixture was poured into 200 mL of THF. Black precipitate (Pt-CNT) was gathered by filtration, washed with water and THF, and then dried in a vacuum oven at 70 ℃ for 12 h.

Pd-Pt CNT: In an oven-dried 500-mL beaker, 100 mg of CNT-ED-OH was dispersed in 200 mL of distilled water. It was then sonicated with an ultrasonicator for 60 min (20 min ×x 3). The dispersion was transferred to 500- mL two-necked reaction flask and bubbled with argon gas for 10 min, then, K_2PdCl_4 (50 mg) dissolved in 10 mL water was slowly added to the

reaction flask. Argon gas was again bubbled through the reaction mixture for 10 min and the mixture was heated to 80 ℃, after which, 10 mL of hydrazine monohydrate was slowly added (4 mL/h) and the mixture was stirred under argon gas (1 atm) for another 12 h. Subsequently, K_2PtCl_4 (50 mg) in 10 mL water was slowly added into the reaction flask. Because of the different standard reduction potentials, we used two separate reducing agents. Because platinum has higher reduction potential than palladium, we used hydrogen gas as a reducing agent. Hydrogen gas was bubbled through the reaction mixture for 1 h, and the mixture was then stirred under hydrogen gas (1 atm) for another 12 h. The mixture was poured into 200 mL of THF. Black precipitate (Pd-Pt-CNT) was gathered by filtration, washed with water and THF, and then dried in a vacuum oven at 70 ℃ for 12 h. The Pd-Pt-CNT was confirmed by transmission electron microscopy (TEM) and energy-dispersive X-ray spectroscopy.

Elemental analysis data CNT-ED-OH. (C,H,N)

- N: 10.3027% C: 49.0364% H: 4.8144% N- 2.45mmol

TEM images of Pd-Pt CNT

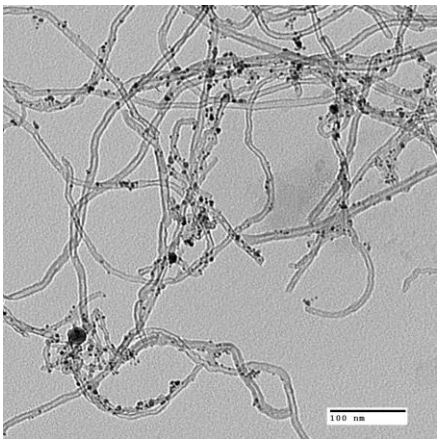

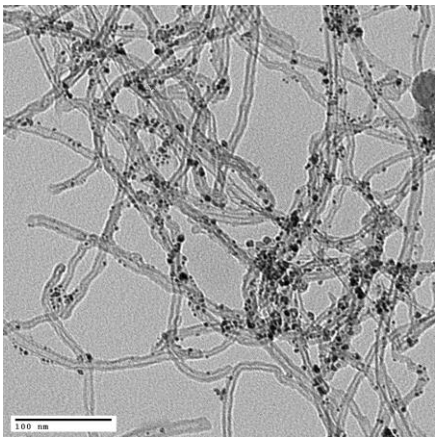

TEM images of Pd-Pt CNT after 11 times of use.

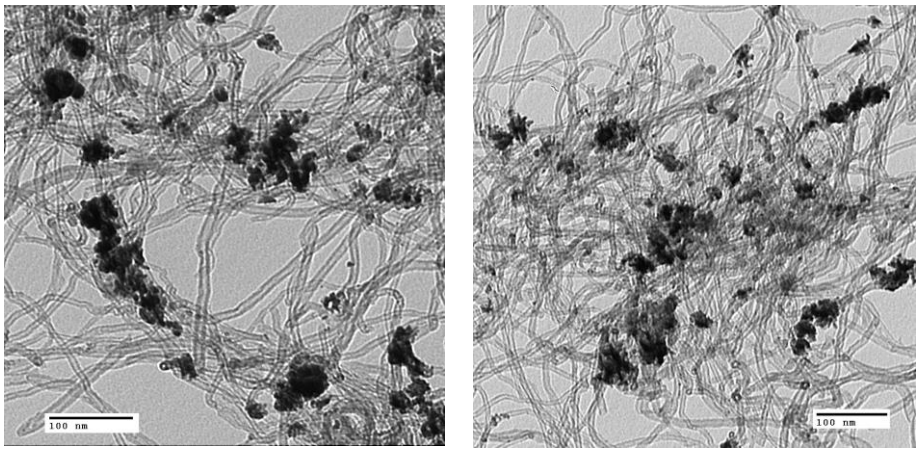

EDS spectrum of Pd-Pt CNT

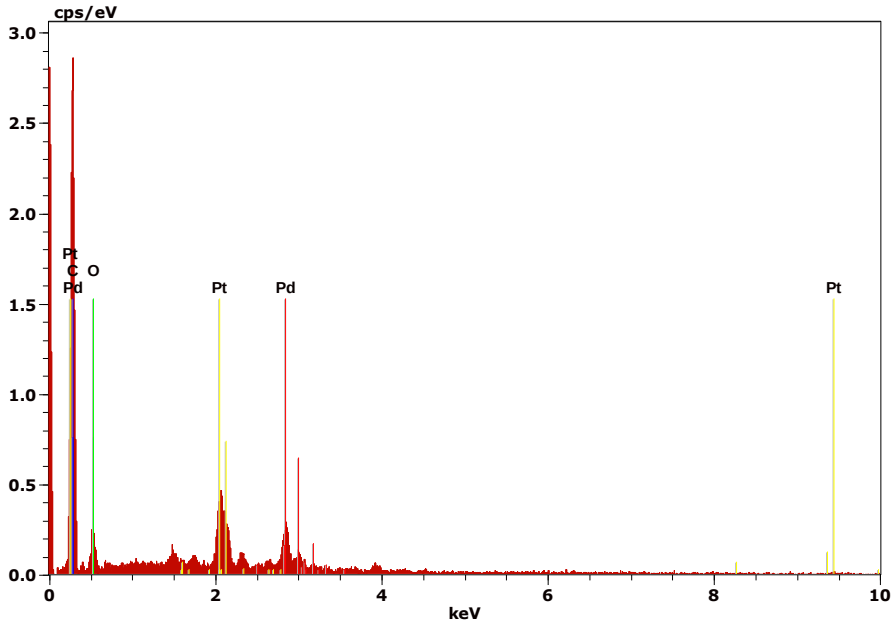

Spectrum: Pd-Pt CNT

Element	Series	unn. C [wt.%]	norm. C [wt.%]	Atom. C [at.%]	Error (3 Sigma) [wt.%]
Palladium	L-series	5.70	8.45	1.25	0.77
Carbon	K-series	43.83	65.05	85.55	19.45
Platinum	M-series	9.64	14.30	1.16	1.34
Oxygen	K-series	8.22	12.19	12.04	5.79

XRD pattern of Pd-Pt CNT

Pd-Pt CNT

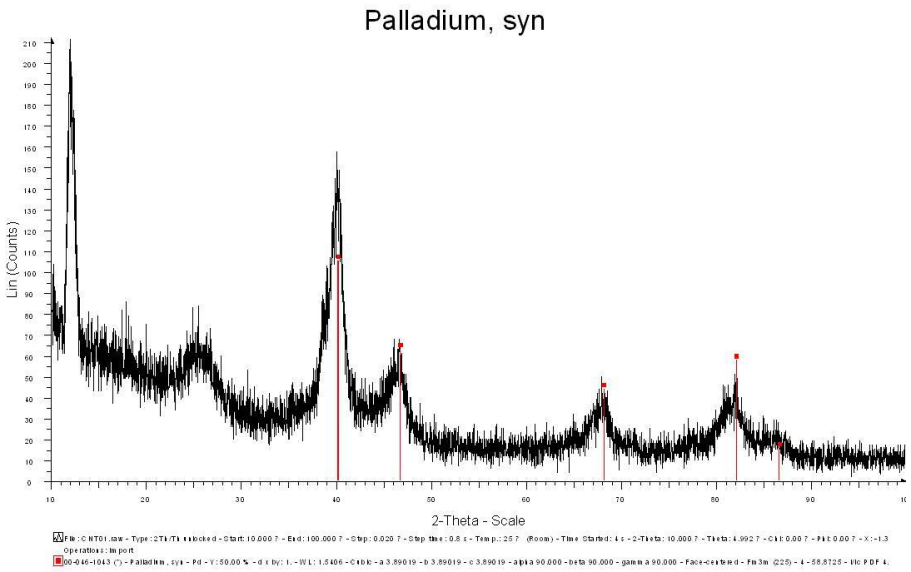

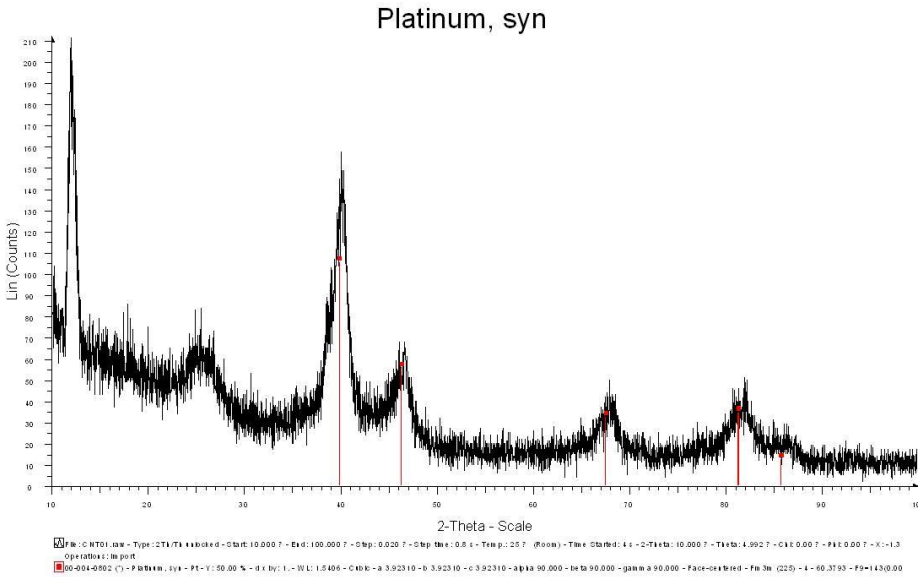

Pd-Pt overlap

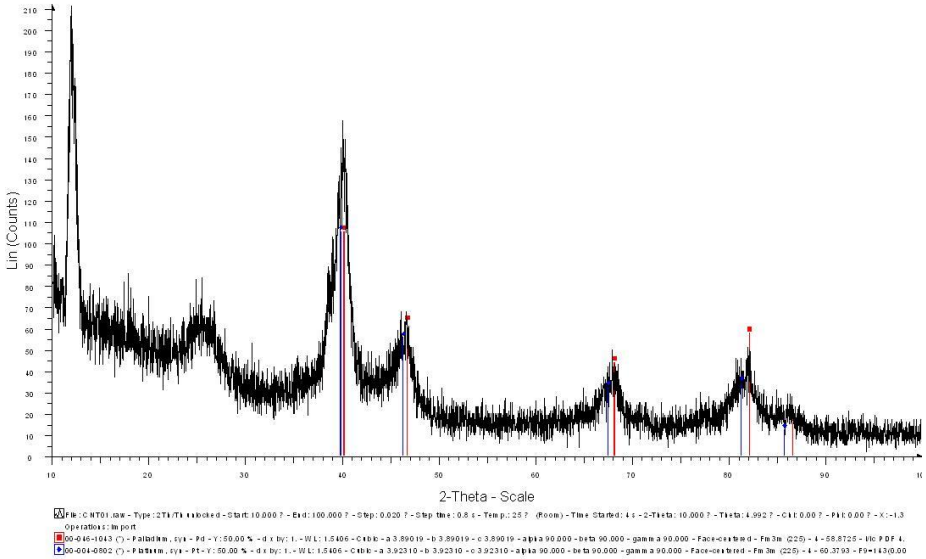

K_2PdCl_4

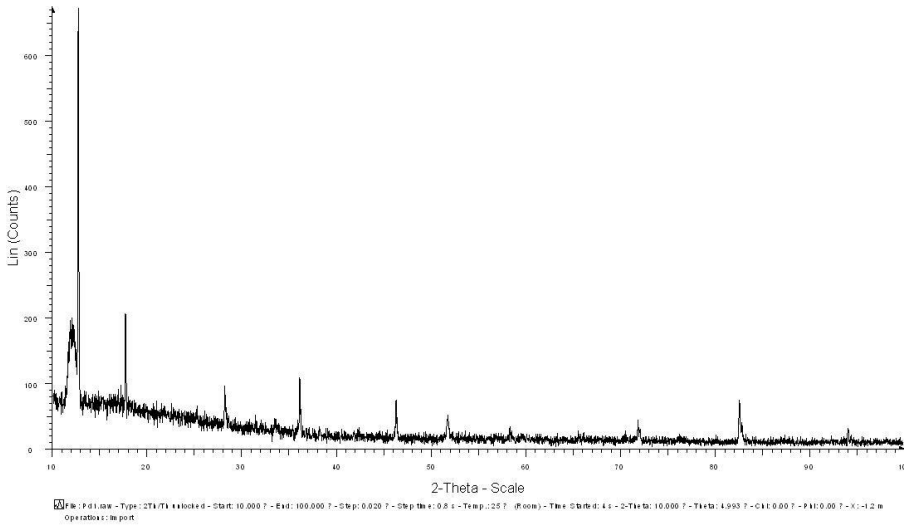

K_2PtCl_4

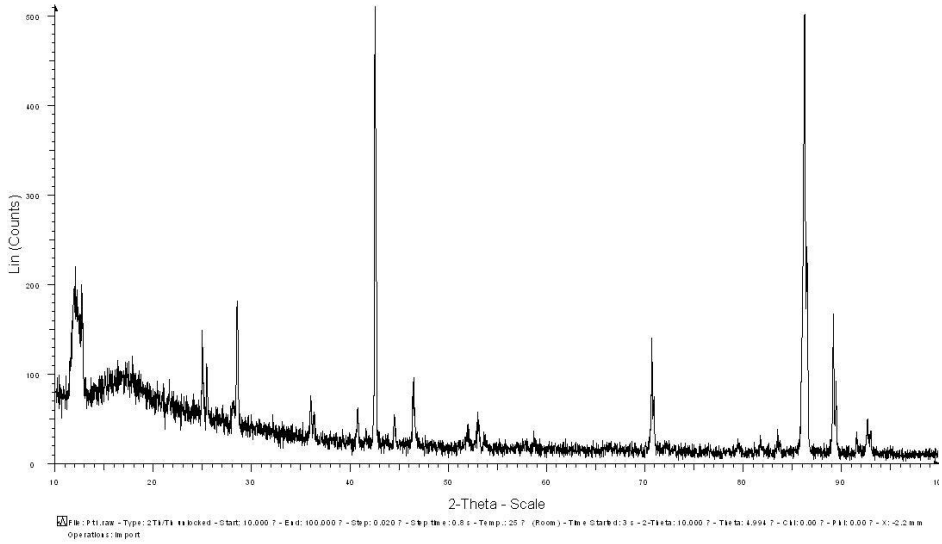

Reference

Part I.

1. A. Wittstock, V. Zielasek, J. Biener, C. M. Friend, Baumer, M. *Science*. **2010**, 327, 319.

2. C. E. Garrett, K. Prasad, *Adv. Synth. Catal*. **2004**, 346, 889.

3. M. T. Reetz, de Vries, J. G. *Chem. Comm*. **2004**, 1559.

4. a) A. T. Bell, *Science*. **2003**, 299, 1688. b) G. A. Somorjai, A. M. Contreras, M. Montano, R. M. Rioux, *Proc. Natl. Acad. Sci*. **2006**, 103, 10577. c) M. Valden, X.Lai, D. W. Goodman, *Science*.**1998**, 281, 1647.

5. B. Koo, H. Xiong, M. D. Slater, V. B. Prakapenka, M. Balasubramanian, P. Podsiadlo, C. S. Johnson, T. Rajh, E. V. Shevchenko, *Nano. Lett*. **2012,** 12, 2429.

6. X. Du, C. Wang, M. Chen, Y. Jiao, J. Wang, *J. Phys. Chem. C* **2009,** 113, 2643.

7. T. Fukushima, K. Sekizaqa, Y. Jin, M. Yamaya, H. Sasaki, T. Takishima, *Am. J. Physiol*. **1993**, 265, L67.

8. Y. R. Chemla, H. L. Crossman, Y. Poon, R. McDermott, R. Stevens, M. D. Alper, J. Clarke, *Proc. Natl. Acad. Sci*. **2000,** USA 97 14268.

9. J. Kim, J. E. Lee, S. H. Lee, J. H. Yu, J. H. Lee, T. G. Park, T. Hyeon, *Adv. Mater*. **2008,** 20, 478.

10. J. Kim, S. Park, J. E. Lee, S. M. Jin, J. H. Lee, I. S. Lee, I. Yang, J. S. Kim, S. K. Kim, M. H. Cho, T. Hyeon, *Angewandte Chemie*. **2006,** 118, 7918.

11. J. Yu, D. Huang, M. Z. Yousaf, Y. Hou, S. Gao, *Chin. Phys. B* **2013**, 22 027506.

12. K. Cheng, S. Peng, C. Xu, S. Sun, *J. Am. Chem. Soc*. **2009,** 131, 10637.

13. a) H. U. Blaser, A. Baiker, R. Prins, *in Heterogeneous Catalysis and Fine Chemicals*; Blaser, H. U.; Schmidt, E. Ed.; Elsevier, Amsterdam **1997**, vol. IV, pp. 17; b) R. S. Downing, P. J. Kunkeler, H. van Bekkum, *Catal. Today* **1997**, *37*, 121; c) S. Cenini, F. Ragaini, *Catalytic Reductive Carbonylation of Organic Nitro Compounds*, Kluwer, Dordrecht, **1996**; d) P. N. Rylander, *Hydrogenation Methods*, Academic Press, London, **1990**; e) S. Nishimura, *Handbook of Heterogeneous Catalytic Hydrogenation for Organic Synthesis*, Wiley, Chichester, **2001**; f) H.-U. Blaser, C. Malan, B. Pugin, F. Spindler, H. Steiner, M. Studer, *Adv. Synth. Catal.*, **2003**, *345*, 103; g) B. Chen, U. Dingerdissen, J. G. E. Krauter, H. G. J. Lansink Rotgerink, K. Möbus, D. J. Ostgard, P. Panster, T. H. Riermeier, S. Seebald, T. Tacke, H. Trauthwein, *Appl. Catal., A*, **2005**, *280*, 17; h) H.-U. Blaser, H. Steiner, M. Studer, *ChemCatChem*, **2009**, *1*, 210; i) A. Corma and H. Garcia, *Chem. Soc. Rev.*, **2008**, *37*, 2096; j) J. P. Adams, J. R. Paterson, *J. Chem. Soc., Perkin Trans. 1*, **2000**, 3695; k) K. Nomura, *J. Mol. Catal. A*, **1998**, *130*, 1; l) G. Wegener, M. Brandt, L. Duda, J. Hofmann, B. Klesczewski, D. Koch, R. Kumpf, H. Orzesek, H. Pirkl, C. Six, C. Steinlein, M. Weisbeck, *Appl. Catal. A* **2001**, *221*, 303.

14. P. Baumeister, H. U. Blaser, M. Studer, *Catal. Lett*. **1997**, *49*, 219.

15. A. Corma, P. Concepción, P. Serna, *Angew. Chem. Int. Ed.*, **2007**, *46*, 7266; b) T. Joseph, K. V. Kumar, A. V. Ramaswamy, S. B. Halligudi, *Catal. Commun.*, **2007**, *8*, 629; c) S. Chandrasekhar, S. J. Prakash, C. L. Rao, *J. Org. Chem.*, **2006**, *71*, 2196; d) P. K. Mandal, J. S. McMurray, *J. Org. Chem.*, **2007**, *72*, 6599; e) N. Pradhan, A. Pal, T. Pal, *Langmuir*, **2001**, *17*, 1800; f) R. J. Rahaim Jr., R. E. Maleczka Jr., *Org. Lett.*, **2005**, *7*, 5087.

16. A. Corma, P. Serna, *Science*, **2006**, *313*, 332; b) Q. Shi, R. Lu, L. Lu, X. Fu, D. Zhao, *Adv. Synth. Catal.*, **2007**, *349*, 1877; c) P. Maity, S. Basu, S. Bhaduri, G. K. Lahiri, *Adv. Synth. Catal.*, **2007**, *349*, 1955; d) A. Corma, P.

Serna, P. Concepción and J. J. Calvino, *J. Am. Chem. Soc.*, **2008**, *130*, 8748; e) J. L. Zhang, Y. Wang, H. Ji, Y. Wei, N. Wu, B. Zuo and Q. Wang, *J. Catal.*, **2005**, *229*, 114; f) P. Serna, P. Concepción and A. Corma, *J. Catal.*, **2009**, *265*, 19; g) C. Yu, B. Liu and L. Hu, *J. Org. Chem.*, **2001**, *66*, 919; h) A. Saha and B. Ranu, *J. Org. Chem.*, **2008**, *73*, 6867; i) M. Takasaki, Y. Motoyama, K. Higashi, S.-H. Yoon, I. Mochida and H. Nagashima, *Org. Lett.*, **2008**, *10*, 1601; j) Y. Motoyama, K. Kamo and H. Nagashima, *Org. Lett.*, **2009**, *11*, 1345; k) Y. Yamane, X. Liu, A. Hamasaki, T. Ishida, M. Haruta, T. Yokoyama and M. Tokunaga, *Org. Lett.*, **2009**, *11*, 5162; l) J. S. D. Kumar, M. M. Ho and T. Toyokuni, *Tetrahedron Lett.*, **2001**, *42*, 5601; m) P. M. Reis and B. Royo, *Tetrahedron Lett.*, **2009**, *50*, 949.

17. a) M. L. Kantam, R. Chakravarti, U. Pal, B. Sreedhar, S. Bhargava, *Adv. Synth. Catal*. **2008**, *350*, 822;b) L. He, L.-C. Wang, H. Sun, J. Ni, Y. Cao, H.-Y. He, K.-N. Fan, *Angew. Chem. Int. Ed*. **2009**, *48*, 9538;

18. J. Lipowitz, S. A. Bowman, *J. Org. Chem*. **1973**, *38*, 162; b) J. Tormo, D. S. Hays, G. C. Fu, *J. Org. Chem.* **1998**, *63*, 5296; c) I. Jovel, L. Golomba, M. Fleisher, J. Popelis, S. Grinberga, E. Lukevics, *Chem. Heterocycle. Compounds* **2004**, *40*, 701;

19. a) A. Furst, R. C. Berlo, S. Hooton, *Chem. Rev*. **1965**, *65*, 51; b) N. R. Ayyangar, A. G. Lugade, P. V. Nikrad, V. K. Sharma, *Synthesis* **1981**, *8*, 640; c) L. P. Kuhn, *J. Am. Chem. Soc*. **1951**, *73*, 1510; d) N. R. Ayyangar, U. R. Kalkote, K. V. Spinvasan, *Synthesis* **1984**, *11*, 938.

20. J. Jankowska, J. Paradowska, J. Mlynarski, *Tetrahedron Lett.* **2006**, *47*, 5281.

21. A. Béchamp, *J. Ann. Chim. Phys*. **1854**, *42*, 186.

22. a) K. Yanada, H. Yamaguchi, R. Yanada, H. Meguri, S. Uchida, *Chem. Lett.* **1989**, 951; b) COUNCIL OF SCIENTIFIC and INDUSTRIAL

RESEARCH Patent: *WO2005/70869 A1*, **2005**; c) D. G. Desai, S. S. Swami, S. K. Dabhade, M. G. Ghagare, *Synth. Commun*. **2001**, *31*, 1249.

23. L. Pehlivan, E. Metay, S. Laval, W. Dayoub, P. Demonchaux, G. Mignani, M. Lemaire, *Tetrahedron Lett*. **2010**, *51*, 1939.

24. K. Junge, B. Wendt, N. Shaikh, M. Beller, *Chem. Commun*. **2010**, *46*, 1769.

25. a) Z.-P. Xiao, Y.-C. Wang, G.-Y. Du, J. Wu, T. Luo, S.-F. Yi, *Synth. Commun*. **2010**, *40*, 661; b) C. Macleod, G. J. McKiernan, E. J. Guthrie, L. J. Farrugia, D. W. Hamprecht, J. Macritchie, R. C. Hartley, *J. Org. Chem*. **2003**, *68*, 387.

26. A. B. Gamble, J. Garner, C. P. Gordon, S. M. O'Conner, P. A. Keller, *Synth. Commun*. **2007**, *37*, 2777.

27. D. Olender, J. Zwawiak, L. Zaprutko, *J. Heterocycl. Chem*. **2010**, *47*, 1049.

28. Y. Liu, Y. Lu, M. Prashad, O. Repic, T. J. Blacklock, *Adv. Synth. Catal*. **2005**, *347*, 217.

29. M. Kumarraja, K. Pitchumani, *Appl. Catal. A* **2004**, *265*, 135.

30. M. Busch, K. Schulz, *Chem. Ber. B62* **1929**, 1458.

31. a) T. Hirashima, O. Manabe, *Chem. Lett*. **1975**, 259; b) B.H. Han, D.H. Shin, *Bull. Korean Chem. Soc*. **1985**, *6*, 320; c) D.L. Clive, A.G. Angoh, B.M. Sharon, *J. Org. Chem*. **1987**, *52*, 1339; d) J. Hine, S. Hahn, D.E. Miles, K. Ahn, *J. Org. Chem*. **1985**, *50*, 5092; e) M. Lauwiner, P. Rys, J. Wissmann, *App. Catal. A* **1998**, *172*, 141; f) M. Benz, A.M.V. Kraan, R. Prins, *App. Catal. A* **1998**, *172*, 149; g) M. Lauwiner, R. Roth, P. Rys, *App. Catal. A* **1999**, *177*, 9; h) P.S. Kumar, J. Sanchez-Valente, F. Figueras, *Tetrahedron Lett*. **1998**, *39*, 2573; i) Q. Shi, R. Lu, K. Jin, Z. Zhang, D. Zhao, *Green Chem*. **2006**, *8*, 868.

32. Y. Jang, S. Kim, S. Jun, B. Kim, S. Hwang, I. Song, B. M. Kim, T. Hyeon *Chem. Commun*., **2011**, *47*, 3601.

33. W. M. N. Ratnayake,; J. S. Grossert,; R. Ackman, *J. Am. Oil. Chem. Soc*. **1990**, 67, 940.

34. (a) C. E. Miller, *J. Chem. Educ*., **1965**, 42, 254. (b) D. J. Pasto; R. T. Taylor, Reductions with Diimide in: Organic Reactions. V.; Paquette, L. A., Ed.; Wiley & Sons: New York, **1991**; Vol. 40, p 91.

35. E. W. Schmidt, Hydrazine and Its Derivatives: Preparation, Properties, and Applications, 2nd ed.; Wiley & Sons: New York, **2001**; Vol. 1, p 475.

36. (a) A. T. Dann; W. Davies, *J. Chem. Soc. (Resumed)*, **1929**, 1050. (b) A. Furst; R. C.Berlo; S. Hooton, *Chem. Rev*. **1965**, 65, 51. (c) P. Lacombe; B. Castagner; Y. Gareau; R. Ruel, *Tetrahedron Lett*. **1998**, 39, 6785. (d) M. H. Haukaas; G. A. O'Doherty, *Org. Lett*. **2002**, 4, 1771. (e) Y. Imada, H. Iida, T. Naota, *J. Am. Chem. Soc*. **2005**, 127, 14544. (f) K. R. Buszek, N. Brown, *J. Org. Chem*. **2007**, 72, 3125. (g) B. J. Marsh, D. R. Carbery, *J. Org. Chem*. **2009**, 74, 3186.

37. (a) W. C. E. Higgison, Recent Aspects of the Inorganic Chemistry of Nitrogen. Chem. Soc., Spec. Publ. **1957**, 10, 95. (b) F. Aylward, M. Sawistowska, *Chem. and Ind*. **1961**, 433. (c) E. J. Corey, W. L. Mock, D. J. Pasto, *Tetrahedron Lett*. **1961**, 2, 347. (d) E. J. Corey, D. J. Pasto, W. L. Mock, *J. Am. Chem. Soc*. **1961**, 83, 2957. (e) S. Hünig, H. R. Müller, W. Thier, *Tetrahedron Lett*. **1961**, 2, 353. (f) F. Aylward, M. Sawistowska, *Chem. and Ind*. **1962**, 484. (g) F. Aylward, M. Sawistowska, *Chem. and Ind*. **1964**, 1435. (h) S. Hünig, H. R Müller; W. Thier, *Angew. Chem. Int. Ed*. **1965**, 4, 271.

38. Ihara Chemical Industry Co., Ltd. JP, 2005/350427A, December 22, 2005.

39. For a review, see; (a) A. Roucoux, J. Schulz, H. Patin, *Chem. Rev*. **2002**, 102, 3757. (b) , J. M. Thomas; B. F. G. Johnson, R. Raja, G. Sankar, P. A. Midgley, *Acc. Chem. Res*. **2003**, 36, 20.

40. (a) M. Shokouhimehr, Y. Piao, J. Kim, Y. Jang, T. Hyeon, *Angew. Chem. Int. Ed*. **2007**, 46, 7039. (b) M.-J. Jin, D.-H Lee, *Angew. Chem. Int. Ed*. **2010**,

49, 1119. (c) A.-H. Lu, W. Schmidt, N. Matoussevitch, H. Bönnemann, B. Spliethoff, B. Tesche, E. Bill, W. Kiefer, F. Schüth, *Angew. Chem. Int. Ed*. **2004**, 43, 4303. (d) A.-H. Lu, E. L. Salabas, F. Schüth, *Angew. Chem. Int. Ed.* **2007**, 46, 1222. (e) Y. Deng, Y. Cai, Z. Sun, J. Liu, C. Liu, J. Wei, W. Li, C. Liu, Y. Wang, D. Zhao, *J. Am. Chem. Soc*. **2010**, 132, 8466. (f) M. Jacinto, J. P. K Kiyohara, S. H. Masunaga, R. F. Jardim, L. M. Rossi, *Appl. Catal. A* **2008**, 338, 52. (g) Z. Yinghuai, S. C. Peng, A. Emi, S. Zhenshun, R. Monalisa, A. Kemp, *Adv. Synth. Catal*. **2007**, 349, 1917. (h) P. D. Stevens, G. Li, J. Fan, M. Yen, Y. Gao, *Chem. Commun*. **2005**, 4435. (i) M. Feyen, C. Weidenthaler, F. Schüth, A.-H. Lu, *Chem. Mater*. **2010**, 22, 2955. (j) L. Aschwanden, B. Panella, P. Rossbach; B. Keller, A. Baiker, *ChemCatChem* **2009**, 1, 111. (k) B. Panella, A.Vargas, A. Baiker, *J. Catal*. **2009**, 261, 88. (l) Y. Zhai, Y. Dou, X. Liu, B. Tu, D. J. Zhao, *Mater. Chem*. **2009**, 19, 3292. (m) P. D Stevens, J. Fan, H. M. R. Gardimalla, M. Yen, Y. Gao, *Org. Lett*. **2005**, 7, 2085. (n) D. Guin, B. Baruwati, S. V. Manorama, *Org. Lett*. **2007**, 9, 1419. (o) B. Baruwati, D. Guin, S. V. Manorama, *Org. Lett*. **2007**, 9, 5377. (p) J. Liu, X, Sun, W. Peng, Y. Zhao, C. Xia, *Org. Lett.* **2008**, 10, 3933. (q) K. Mori, Y. Kondo, H. Yamashita, *Phys. Chem. Chem. Phys*. **2009**, 11, 8949.

41. E. J. Corey, D. J. Pasto, W. L. Mock, *J. Am. Chem. Soc*. **1961**, *83*, 2957.

42. J. W. Larsen, M. Freund, K. Y. Kim, M. Sidovar, J. L. Stuart, *Carbon* **2000**, *38*, 655.

43. a) B. H. Han, D. H. Shin, S. Y. Cho, *Tetrahedron Lett*. **1985**, *26*, 6233; b) G. R. Srinisava, K. Abiraj, D. C. Gowda, *Ind. J. Chem. Sect. B* **2003**, *42*, 2885; c) S. Gowda, D. C. Gowda, *Ind. J. Chem. Sect. B* **2003**, *42*, 180; d) M. G. Banwell, A. J. Edwards, K. A. Jolliffe, M. Kemmler, *J. Chem. Soc. Perkin Trans. 1* **2001**, *12*, 1345; e) P. K. Arora, A. P. Bhaduri, Ind. *J. Chem. Sect. B* **1981**, *20*, 951; f) D. H. Lloyd, D. E. Nicholas, *J. Org. Chem.* **1986**, *51*, 4294;

Part II.

1. S. Iijima, *Nature*, **1991**, 354, 56.

2. Y.-A. Lv, Y.-H. Cui, Y.-Z. Xiang, J.-G. Wang, X.-N. Li, *COMP MATER SCI* **2010**, 48, 621.

3. A. Javey, J. Guo, Q. Wang, M. Lundstrom, H. Dai, *Nature* **2003**, 424, 654.

4. A. K. Geim, K. S. Novoselov, *Nat. Mater*. **2007**, 6, 183.

5. S. Berber, Y.-K. Kwon, D. Tománek, *Phys. Rev. Lett*. **2000**, 84, 4613.

6. J. H. Seol, I. Jo, A. L. Moore, L. Lindsay, Z. H. Aitken, M. T. Pettes, X. Li, Z. Yao, R. Huang, D. Broido, N. Mingo, R. S. Ruoff, L. Shi, *Science* **2010**, 328, 213.

7. A. Peigney, C. Laurent, E. Flahaut, R. R. Bacsa, A. Rousset, *Carbon* **2001**, 39, 507.

8. C. N. R. Rao, A. K. Sood, K. S. Subrahmanyam, A. Govindaraj, *Angew. Chem. Int. Ed*. **2009**, 48, 7752.

9. M.-F. Yu, O. Lourie, M. J. Dyer, K. Moloni, T. F. Kelly, R. S. Ruoff, *Science* **2000**, 287, 637.

10. C. Lee, X. Wei, J. W. Kysar, J. Hone, *Science* **2008**, 321, 385.

11. P. Avouris, *Nano Lett*. **2010**, 10, 4285.

12. A. H. Castro Neto, F. Guinea, N. M. R. Peres, K. S. Novoselov, A. K. Geim, *Rev. Mod. Phys*. **2009**, 81, 109.

13. S. Gupta, K. Dharamvir, V. K. Jindal, *Phys. Rev. B* **2005**, 72, 165428.

14. Q. Cao, H.-s. Kim, N. Pimparkar, J. P. Kulkarni, C. Wang, M. Shim, K. Roy, M. A. Alam, J. A. Rogers, *Nature* **2008**, 454, 495.

15. M. Zhang, S. Fang, A. A. Zakhidov, S. B. Lee, A. E. Aliev, C. D. Williams, K. R. Atkinson, R. H. Baughman, *Science* **2005**, 309, 1215.

16. K. S. Kim, Y. Zhao, H. Jang, S. Y. Lee, J. M. Kim, K. S. Kim, J.-H. Ahn, P. Kim, J.-Y. Choi, B. H. Hong, *Nature* **2009**, 457, 706.

17. S. K. Hwang, J. M. Lee, S. Kim, J. S. Park, H. I. Park, C. W. Ahn, K. J. Lee, T. Lee, S. O. Kim, *Nano Lett*. **2012**, 12, 2217.

18. T. Georgiou, R. Jalil, B. D. Belle, L. Britnell, R. V. Gorbachev, S. V. Morozov, Y.-J. Kim, A. Gholinia, S. J. Haigh, O. Makarovsky, L. Eaves, L. A. Ponomarenko, A. K. Geim, K. S. Novoselov, A. Mishchenko, *Nat. Nanotechnol*. **2013**, 8, 100.

19. S.-K. Lee, H. Y. Jang, S. Jang, E. Choi, B. H. Hong, J. Lee, S. Park, J.-H. Ahn, *Nano Lett*. **2012**, 12, 3472.

20. D. H. Choi, Q. Wang, Y. Azuma, Y. Majima, J. H. Warner, Y. Miyata, H. Shinohara, R. Kitaura, *Sci. Rep*. **2013**, 3.

21. S.-C. J. Huang, A. B. Artyukhin, N. Misra, J. A. Martinez, P. A. Stroeve, C. P. Grigoropoulos, J.-W. W. Ju, A. Noy, *Nano Lett*. **2010**, 10, 1812.

22. M. F. El-Kady, V. Strong, S. Dubin, R. B. Kaner, *Science* **2012**, 335, 1326.

23. A. L. M. Reddy, A. Srivastava, S. R. Gowda, H. Gullapalli, M. Dubey, P. M. Ajayan, *ACS Nano* **2010**, 4, 6337.

24. S. H. Lee, H. W. Kim, J. O. Hwang, W. J. Lee, J. Kwon, C. W. Bielawski, R. S. Ruoff, S. O. Kim, *Angew. Chem. Int. Ed*. **2010**, 49, 10084.

25. S.W. Lee, N. Yabuuchi, B. M. Gallant, S. Chen, B.-S. Kim, P. T. Hammond, Y. Shao-Horn, *Nat. Nanotechnol*. **2010**, 5, 531.

26. K. S. Lee, W. J. Lee, N.-G. Park, S. O. Kim, J. H. Park, *Chem. Commun*. **2011**, 47, 4264.

27. D. H. Lee, W. J. Lee, W. J. Lee, S. O. Kim, Y.-H. Kim, *Phys. Rev. Lett*. **2011**, 106, 175502.

28. K. Gong, F. Du, Z. Xia, M. Durstock, L. Dai, *Science* **2009**, 323, 760.

29. G. F. Zou, H. M. Luo, S. Baily, Y. Y. Zhang, N. F. Haberkorn, J. Xiong, E. Bauer, T. M. McCleskey, A. K. Burrell, L. Civale, Y. T. Zhu, J. L. MacManus-Driscoll, Q. X. Jia, *Nat. Commun*. **2011**, 2, 428.

30. P. M. Ajayan, O. Stephan, C. Colliex, D. Trauth, *Science* **1994**, 265, 1212.

31. A. B. Dalton, S. Collins, E. Munoz, J. M. Razal, V. H. Ebron, J. P. Ferraris, J. N. Coleman, B. G. Kim, R. H. Baughman, *Nature* **2003**, 423, 703.

32. W. J. Lee, J. M. Lee, S. T. Kochuveedu, T. H. Han, H. Y. Jeong, M. Park, J. M. Yun, J. Kwon, K. No, D. H. Kim, S. O. Kim, *ACS Nano* **2011**, 6, 935.

33. S. Stankovich, D. A. Dikin, G. H. B. Dommett, K. M. Kohlhaas, E. J. Zimney, E. A. Stach, R. D. Piner, S. T. Nguyen, R. S. Ruoff, *Nature* **2006**, 442, 282.

34. C. A. Dyke, J. M. Tour, *J. Phys. Chem. A*, **2004**, *108*, 11151.

35. (a) J. L. Bahr, J. Yang,; D. V. Kosynkin, M. J. Bronikowski, R. E. Smalley, J. M. Tour, *J. Am. Chem. Soc.* **2001**, *123*, 6536; (b) J. L. Bahr, J. M. Tour, *Chem. Mater.* **2001**, *13*, 3823; (c) C. A. Dyke, J. M. Tour, *Nano Lett.* **2003**, *3*, 1215; (d) C. A. Dyke, J. M. Tour, *J. Am. Chem. Soc.* **2003**, *125*, 1156; (e) J. L. Stephenson, S. Hudson, Azad, J. M. Tour, *Chem. Mater*. **2006**, *18*, 374; (f) Z.-Z Zhua, Z. Wang, H.-L. Li, *J. Power Sources* **2009**, *186*, 339.

36. J. L. Hudson.; M. J. Casavant, J. M. Tour, *J. Am. Chem. Soc.* **2004**, *126*, 11158.

37. E. T Mickelson, C. B. Huffman, A. G. Rinzler, R. E. Smalley, R. H. Hauge, J. L. Margrave, *Chem. Phys. Lett.* **1998**, *296*, 188.

38. Y. Ying, R. K. Saini, F. Liang, A. K. Sadana, W. E. Billups, *Org. Lett.* **2003**, *5*, 1471.

39. F. Liang,; A. K. Sadana, A. Peera, J. Chattopadhyay, Z, Gu, R. H. Hauge, W. E. Billups, *Nano Lett.* **2004**, *4*, 1257.

40. V. Georgakilas, K. Kordatos, M. Prato, D. M. Guldi, M. Holzinger, A. Hirsch, *J. Am. Chem. Soc.* **2002**, *124*, 760.

41. M. Holzinger, J. Abraham, P. Whelan, R. Graupner, L. Ley, F. Hennrich, M. Kappes, A. Hirsch, *J. Am. Chem. Soc.* **2003**, *125*, 8566.

42. K. S. Coleman, S. R. Bailey, S. Fogden, M. L. H. Green, *J. Am. Chem. Soc.* **2003**, *125*, 8722.

43. M. Holzinger, J. Steinmetz, D. Samaille, M. Glerup, M. Paillet, P. Bernier, L. Ley, R. Graupner, *Carbon* **2004**, *42*, 941.

44. M. Tunckol, S. Fantini, F. Malbosc, J. Durand, P. Serp, *Carbon* **2013,** 57, 209.

45. A. Hirsch, *Angew. Chem. Int. Ed* **2002,** 41, 1853.

46. M. Holzinger, O. Vostrowsky, A. Hirsch, F. Hennrich, M. Kappes, R. Weiss, F. Jellen, *Angew. Chem. Int. Ed* **2001,** 40, 4002.

47. C. Gao, H. He, L. Zhou, X. Zheng, Y. Zhang, *Chem Mater* **2009**, 21, 360.

48. Y. Jiang, C. Jin, F. Yang, X. Yu, G. Wang, S. Cheng, Y. Di, J. Li, D. Fu, Q. Ni, *J Nanopart Res* **2011**,13, 33.

49. D. R. Shobha Jeykumari, S. S. Narayanan, *Carbon* **2009**, 47, 957

50. X. Yu, D. Chattopadhyay, I. Galeska, F. Papadimitrakopoulos, J. F. Rusling, *Electrochem Commun* **2003,** 5, 408.

51. J. M. Gomez, M. D. Romero, T. M. Fernandez, *Catal Lett* **2005**, 101, 275.

52. Q. Shi, D. Yang, Y. Su, J. Li, Z. Jiang, Y. Jiang, W. Yuan, *J Nanopart Res* **2007**, 9 1205.

53. M. Salavati-Niasari, M. Bazarganipour, *Appl Surf Sci* **2008,** 255, 2963.

54. C. Baleizao, B. Gigante, H. Garcia, A. Corma, *J Catal* **2004**, 221, 77.

55. Y. H. Lin, F. Lu, Y. Tu. Z. F. Ren, Nano Lett **2004,** 4, 191.

56. Y. Wang, Z. Iqbal, S.V. Malhotra, *Chem Phys Lett* **2005,** 402, 96.

57. B. Wu, Y. Kuang, X. Zhang, J. Chen, *Nano Today* **2011**, 6, 75.

58. K. Wua, X. Mao, Y. Liang, Y. Chen, Y. Tang, Y. Zhou, J. Lin, C. Mab, T. Lu, *J Power Source* **2012**, 219, 258.

59. Z. Zheng, Y. Du, Z. Wang, Q. Fenga, C. Wang *Analyst* **2013**, 138, 693.

60. B. H. Zhao, J. G. Chen, X. Liu, Z. W. Liu, Z. Hao, J. Xiao, Z. T. Liu, *Ind Eng Chem Res* **2012**, 51, 11112.

61. Y. C. Lin, J. H. Lin, *Catal Commun* **2013**, 34, 41.

62. J. Ziebro, B. Skorupińska, G. Kądziołka, B. Michalkiewicz, *Fuller*

Nanotub Car N **2013,** 21, 333.

63. M. Scarselli, L. Camilli, P. Castrucci, F. Nanni, S. DelGobbo, E. Gautron, S. Lefrant, M.D. Crescenzi, *Carbon* **2012**, 50, 875.

64. E. Antolini, *Applied Catalysis B: Environmental* **2009**, 88, 1.

65. A. Corma, H. Garcia, A. Leyva, *J Mol Catal A-Chem* **2005**, 230, 97.

66. F. Cheng, A. Adronov, *Chem Mater* **2006**, 18, 5389.

67. H. B. Pan, C. H. Yen, B. Yoon, M. Sato, C. M. Wai, *Synthetic Commun* **2006,** 36, 3473.

68. N. Karousis, G.E. Tsotsou, F. Evangelista, P. Rudolf, N. Ragoussis, N. Tagmatarchis, *J Phys Chem C* **2008**, 112, 13463.

69. X. Chen, Y. Hou, H. Wang, Y. Cao, J. He, *J Phys Chem C* **2008**, 112, 8172.

70. P.P. Zhang, X.X. Zhang, H.X. Sun, R.H. Liu, B. Wang, Y.H. Lin, *Tetrahedron Lett* **2009**, 50, 4455.

71. J. A. Sullivan, K. A. Flanagan, H. Hain, *Catal Today* **2009**, 145, 1083.

72. Z. M. Peng, H. Yang, *Nano Today* **2009**, 4, 143.

73. B. K. Lim, M. J. Jiang, P. H. C. Camargo, E. C. Cho, J. Tao, X. M. Lu, Y. M. Zhu, Y. A. Xia, *Science* **2009**, 324, 1302.

74. R. Ferrando, J. Jellinek, R. L. Johnston, *Chem Rev* **2008**, 108, 845.

75. C. J. Serpell, J. Cookson, D. Ozkaya, P. D. Beer, *Nature Chem* **2011**, 3, 478.

76. M. C. Daniel, D. Astruc, *Chemical Rev* **2004**, 104, 293.

77. S. Alayoglu, P. Zavalij, B. Eichhorn, Q. Wang, A. I. Frenkel, P. Chupas, *ACS Nano* **2009**, 3, 3127.

78. S. Alayoglu, A. U. Nilekar, M. Mavrikakis, B. Eichhorn, *Nature Mater* **2008**, 7, 333.

79. F. Tao, M. E. Grass, Y. W. Zhang, D. R. Butcher, F. Aksoy, S. Aloni, V. Altoe, S. Alayoglu, J. R. Renzas, C. K. Tsung, Z. W. Zhu, Z. Liu, M. Salmeron, G. A. Somorjai, *J. Am. Chem. Soc.* **2010**, 132, 8697.

80. Q. Yuan, Z. Y. Zhou, J. Zhuang, and X. Wang, *Chem Commun* **2010**, 46, 1491.

81. Y. Li, T. Kaneko, T. Ogawa, M. Takahashi, R. Hatakeyama, *Chem Commun* **2007**, 3, 254.

82. V. Georgakilas, D. Gournis, V. Tzitzios, L. Pasquato, D. M. Guldi, M. Prato, *J Mater Chem* **2007**, 17, 2679.

83. D. Eder, *Chem Rev* **2010**, 110, 1348.

84. H. B. Pan, C. M. Wai, *New J Chem* **2011**, 35, 1649.

85. S. Ghosh, R. K. Sahu, C. R. Raj, *Nanotechnology* **2012**, 23, 385602.

86. P. H. Liao, H. M. Yang, *Catal Lett* **2008,** 121, 274.

87. M. Tafesh, J. Weiguny, *Chem Rev* **1996**, 96, 2035.

88. S. K. Mohapatra, S. U. Sonavane , R. V. Jayaram, P. Selvam, *Appl Catal B* **2003**, 46, 155.

89. Béchamp, *Annales de chimie Chimie et de physique Physique* **1854**, 42, 186.

90. A. Corma, P. Concepción, P. Serna, *Angew. Chem. Int. Ed* **2007**, 46, 7266.

91. L. He, L.-C. Wang, H. Sun, J. Ni, Y. Cao, H.-Y. He, K.-N. Fan, *Angew. Chem. Int. Ed* **2009**, 48, 9538.

92. J. Tormo, D. S. Hays, G. C. Fu, *Angew. Chem. Int. Ed* **1998**, 63, 5296.

93. Q. Shi, R. Lu, K. Jin, Z. Zhang, D. Zhao, *Green Chem* **2006**, 8, 868.

94. Y. Jang, S. Kim, S. W. Jun, B. H. Kim, S. Hwang, I. K. Song, B. M. Kim, T. Hyeon, *Chem Commun* **2011**, 47, 3601.

95. (a) J. Shen, W. Huang, L. Wu, Y. Hu, M. Ye, *Mater. Sci. Eng. A* **2007**, *464*, 151; (b) X. H. Men, Z. Z. Zhang, H. J. Song, K. Wang, W. Jiang, *Comp. Sci. Technol*. **2008**, *68*, 1042; (c) H. Kitano, K. Tachimoto, Y. J. Anraku, *Colloid Interface Sci*. **2007**, *306*, 28; (d) W. Song, Z. Zheng, W. Tang, X. Wang, *Polymer* **2007**, *48*, 3658; (e) X. Chen, H. Shimizu, *Polymer* **2008**, *49*, 943; (f) N. A. Kumar, H. S. Ganapathy, J. S. Kim, Y. S. Jeong, Y. T. Jeong,

Eur. Polym. J. **2008**, *44*, 579; (g) S. Kumar, R. Kumar, V. K. Jindal, L. M. Bharadwaj, *Mater. Lett.* **2008**, *62*, 731.

96. X. L. Xie, Y. –W. Mai, X. –P. Zhou, *Mater. Sci. Eng. R* **2005**, *49*, 89.

97. J. Y. Choi, S. –W. Han, W. –S. Huh, L. –S. Tan, J. B. Baek, *Polymer* **2007**, *48*, 4034.

98. A. M. Shanmugharaj, J. H. Bae, K. Y. Lee, W. H. Noh, S. H. Lee, S. H. Ryu, *Comp. Sci. Technol.* **2007**, *67*, 1813.

99. J. Jin, Z. Dong, J. He, R. Li, J. Ma, *Nanoscale Res Lett*. **2009**, 7.

100. M. Taki, M. Desaki, A. Ojida, S. Iyoshi, T. Hirayama, I. Hamachi, Y. Yamamoto, *J. Am. Chem. Soc.* **2008**, *130*, 12564.

101. C. Grandjean, A. Boutonnier, C. Guerreiro, J.-M. Fournier, L. A. Mulard, *J. Org. Chem.* **2005**, *70*, 7123.

102. T. Zhang, M. Xu, L. He, K. Xi, M. Gu, Z. Jiang, *Carbon*. **2008**, *46*, 1782

국문초록

I. 산화철 나노 입자들을 이용한 효과적이고 선택적인 재사용 반응

나이트로와 올레핀 환원 반응은 유기 반응 중 가장 기본적이고 중요한 반응 중에 하나이다. 일반적으로 보통의 환원 반응조건은 불균일 촉매를 사용한다. 흔히 쓰는 불균일 촉매의 종류에는 팔라듐 착콜, 로디움 착콜, 플레티늄 착콜이나 라니 니켈등이 있고 보통 수소 기체를 통하여 환원 반응을 진행하게 된다. 이 연구는 그 동안 알려진 촉매와는 달리 산화철 나노입자를 사용하여 더 효율적인 반응에 대해 연구를 진행하였다. 특히 쉽게 구입할 수 있는 산화철 나노입자 촉매를 가지고 나이트로 환원 반응을 진행하였다. 하이드라진 수화물을 환원제로 사용하고 20 mol%의 산화철 나노 입자를 사용했을 때 반응이 가장 효율적으로 진행되었고 반응이 끝난 후에는 산화철 나노 입자의 자성을 이용하여 쉽게 분리해 낼 수 있었다. 분리해 낸 나노 입자를 세척한 후 반응에 재사용할 수 있었고 10번까지 반응성이 떨어지지 않는 높은 수득율을 얻을 수 있었으며 다른 부반응 생성물도 나타나지 않았다. 또한 일반적으로 환원 반응하에서 깨지기 쉬운 할로젠, 에스터, 벤질과 같은 그룹들 존재하에도 문제 없이 나이트로 반응이 진행되는 것을 확인할 수 있었다. 게다가 같은 산화철 나노 촉매를 가지고 올레핀 그룹의 환원 반응도 진행할 수 있었고 역시 10번째까지 전혀 문제 없이 올레핀 반응을 진행시킬 수 있었다. 이와 같은 산화철 나노 입자 촉매를 이용해 선택적이고 효율적인 새로운 촉매반응에 대해 연구할 수 있었다.

II. 다중벽 탄소 나노튜브를 이용한 표면화와 촉매반응에 대한 연구

탄소나노 튜브는 산업적으로 다양한 분야에 사용될 수 있다. 이를 위해서는 나노 튜브 표면에 원하는 작용기를 선택적으로 도입하는 것이 필요하다. 작용기를 도입하기 위한 방법으로 다이아조늄 염을 생성하여 도입하는 방법과 아자이드 화합물로부터 나이트린을 형성하여 나노 튜브 표면에 아지리딘을 형성하는 나이트린 반응 두 가지 방법을 주로 사용하였다. 그 중 특히 나이트린 반응을 이용한 방법은 탄소 나노 튜브의 물리적인 성질을 유지할 수 있어서 용이하다. 이와 같은 나이트린 반응을 이용하여 아민이나 하이드록시기, 카르복시기, 피리딘과 같은 형대의 작용기들을 도입할 수 있었다. 여기에 금속 염의 수용액과 환원제를 통해 환원하여 탄소 나노 튜브 유도체에 고정화를 시도하였다. 환원되는 금속의 환원 준위에 따라 팔라듐은 하이드라진, 플래티늄은 수소기체를 통해 금속 나노 입자들을 탄소 나노 튜브에 고정하였다. 완성된 팔라듐-탄소 나노튜브는 Suzuki coupling 반응에 대해 좋은 반응성을 보였다. 반응이 끝난 후 필터하고 건조시켜 추가적인 재사용이 가능하였다. 팔라듐-탄소 나노튜브는 최소 7번째까지 반응성이 떨어지지 않고 사용이 가능하였다. 추가적으로 탄소 나노 튜브의 풍부한 전자 시스템을 이용하기 위한 산화 환원 반응을 시험해보기 위해 팔라듐 탄소 나노 튜브에 추가적으로 플래티늄 염 수용액을 통해 이원 금속 촉매 시스템을 개발하였다. 팔라듐-플래티늄 이원 금속 탄소 나노 튜브 촉매를 가지고 나이트로 환원 반응을 진행하였다. 팔라듐과 플래티늄 단일 금속 탄소 나노 촉매과는 달리 이원 금속 탄노 나노 튜브 촉매에서 훨씬 더 좋은 반응성을 보였다. 이와 같은 조건하에서 다양한 나이트로 화합물들을 환원 시켜 보았고 수소화 반응에서 쉽게 깨지기 쉬운 작용기를 가진 화합물들도 문제 없이 환원 반응을 진행할 수 있었다. 추가적으로 같은 조건하에서 올레핀 계열의 화합물들도

반응이 잘 진행되었다. 반응이 끝난 후 이원 금속 탄소 나노 튜브 촉매를 필터하여 건조한 후 재사용하였고, 10번까지 반응성이 떨어지지 않는 것을 확인하였다.